PRESSURE FIELD DUE TO UNSTEADY LOADING OF A MARINE PROPELLER

Jorge Roque de D'Almeida

PRESSURE FIELD DUE TO UNSTEADY LOADING

OF A MARINE PROPELLER

by

Jorge Roque de Pinho D'Almeida

B.S., Escola Naval (Portugal)
(1965)

Submitted in partial fulfillment

of the requirements for the

Degrees of Naval Engineer

and

Master of Science

in Naval Architecture and Marine Engineering

at the

Massachusetts Institute of Technology

May, 1971

(1)

ABSTRACT

Title: PRESSURE FIELD DUE TO UNSTEADY LOADING OF A MARINE PROPELLER

Author: J.R.P. D'Almeida

Submitted to the Department of Naval Architecture and Marine Engineering on May 14, 1971, in partial fulfillment of the requirements for the degrees of Naval Engineer and Master of Science in Naval Architecture and Marine Engineering.

A vortex model is used to develop a scheme to compute the pressure field around a marine propeller operating in a wake which is nonuniform in both the radial and circumferential directions. This model takes into account the effects of thickness form and outline of the blades and the form of the unsteady loading distribution, both radially and over the chord. The model can be used for lightly as well as "moderately" loaded propellers. Following the theoretical development a computer program is written in FORTRAN IV, to be used with the IBM System/360-65 digital computer. The workability of the program is tested with sample calculations.

Thesis Supervisor: Justin E. Kerwin

Title: Professor of Naval Architecture

ACKNOWLEDGMENT

The author wishes to express his indebtedness to Professor Justin E. Kerwin for his help and guidance without which this thesis could not have been done.

The author would also like to thank Dr. Stavros Tsakonas for helping to clarify certain aspects of this work and Mrs. Aimée Károlyi for typing the manuscript.

TABLE OF CONTENTS

LIST OF FIGURES

LIST OF TABLES

NOTATION

K	=	Number of blades of the propeller
k_n	=	Reduced frequency
K_p	=	Nondimensional pressure coefficient, $K_p = \dfrac{\Delta p}{4\rho_f (RPM/60)^2 R^2}$
ℓ	=	Blade section length
N	=	Harmonic number
NT	=	Nondimensional time, $NT = t \times RPM/60$
P	=	Pitch in general
Δp	=	Pressure jump in general
R	=	Propeller radius
r_h	=	Hub radius
RPM	=	Propeller revolutions per minute
s,r,n	=	Curvilinear coordinate system defined in Fig. 2.
T	=	Maximum thickness of propeller blade section
t	=	Time variable
u_a	=	Axial perturbation velocity in general
u_t	=	Tangentical perturbation velocity in general
V_o	=	Relative flow past a blade section
V_s	=	Ship speed
x,r,θ	=	Cylindrical coordinate system defined in Fig. 2
x,y,z	=	Cartesian coordinate system defined in Fig. 2
β	=	Advance angle
γ	=	Circulation in general
δ_k	=	A coordinate of tip of k'th blade

λ =   Advance coefficient

θ_L = θ coordinate of leading edge

θ_T = θ coordinate of trailing edge

Ω =   Propeller angular velocity

Φ =   Velocity potential in general

ρ_f =   Fluid density

τ =   Blade section thickness

ξ, ρ, φ =   Dummy cylindrical coordinates

ξ, η, ζ =   Dummy cartesian coordinates

Note: Other symbols and abbreviations are explained whenever used.

Chapter I

INTRODUCTION

The propeller induced vibratory forces acting on a ship have been for a long time an important subject of experimental and theoretical research. Although some important conclusions have been reached based on reliable experimental results [17], it is always hard, if not impossible, to support such conclusions with theoretical calculations. One reason for this defficiency is that for a long time no analytical method was available for evaluating the propeller loading as a three-dimensional problem.

The initial numerical results obtained for the propeller-induced pressure field were based on a simple lifting-line representation [10] which was found to predict pressures far below those obtained from measurement. This theory was later refined by including the effect of the blade thickness and this brought the numerical results closer to the experimental data [9, 10, 11].

The effects on the pressure field due to nonuniform inflow were studied by Tsakonas et al. [8]. They treated the problem as a Dirichlet problem of potential theory and related the pressure field near the propeller to the trust- and torque-producing forces. These forces were computed using the gust theory for airfoil, and assuming that the flow around each blade was two-dimensional. Two correction factors were added to compensate for cascade and finite aspect ratio effects. Even though the calculations made using this method cannot be considered very accurate, they can give an idea of the relative importance

of the unsteady effects arising from the nonuniformity of the ship's wake. This can be seen in Fig. 1, taken from [8]. It is apparent that very close to the plane of the propeller the increase in pressure due to nonuniformity is at most 20 percent of the total pressure but beyond x/D = 0.4 the percentage change becomes much greater. The reason is that at such distances all the pressures are small, but the slow rate of decay of the components arising from nonuniformity makes them more important. It must be noted, however, that the pressure due to thickness is not included in Fig. 1 so that the relative effect close to the propeller arising from nonuniform inflow is of the order of 10 percent for the particular wake used in these calculations.

A truly three-dimensional theory was recently used by Kerwin [18] to compute the field point velocities induced by a marine pro-peller operating in a steady flow. He makes use of the vortex theory to represent the blade loading and derives a scheme to compute the per-turbation velocities on specified field points located on the blades.

In the present work we will extend the program developed by Professor Kerwin to include field points located at any point in the fluid around the propeller and to take into account the unsteady effects due to a nonuniform inflow such as is found in a ship's wake. In addition, a scheme will be developed to compute the velocity potential at the field points. The pressure field is then computed by sub-stituting the perturbation velocities and time variation of the velocity potential into Bernoulli's equation.
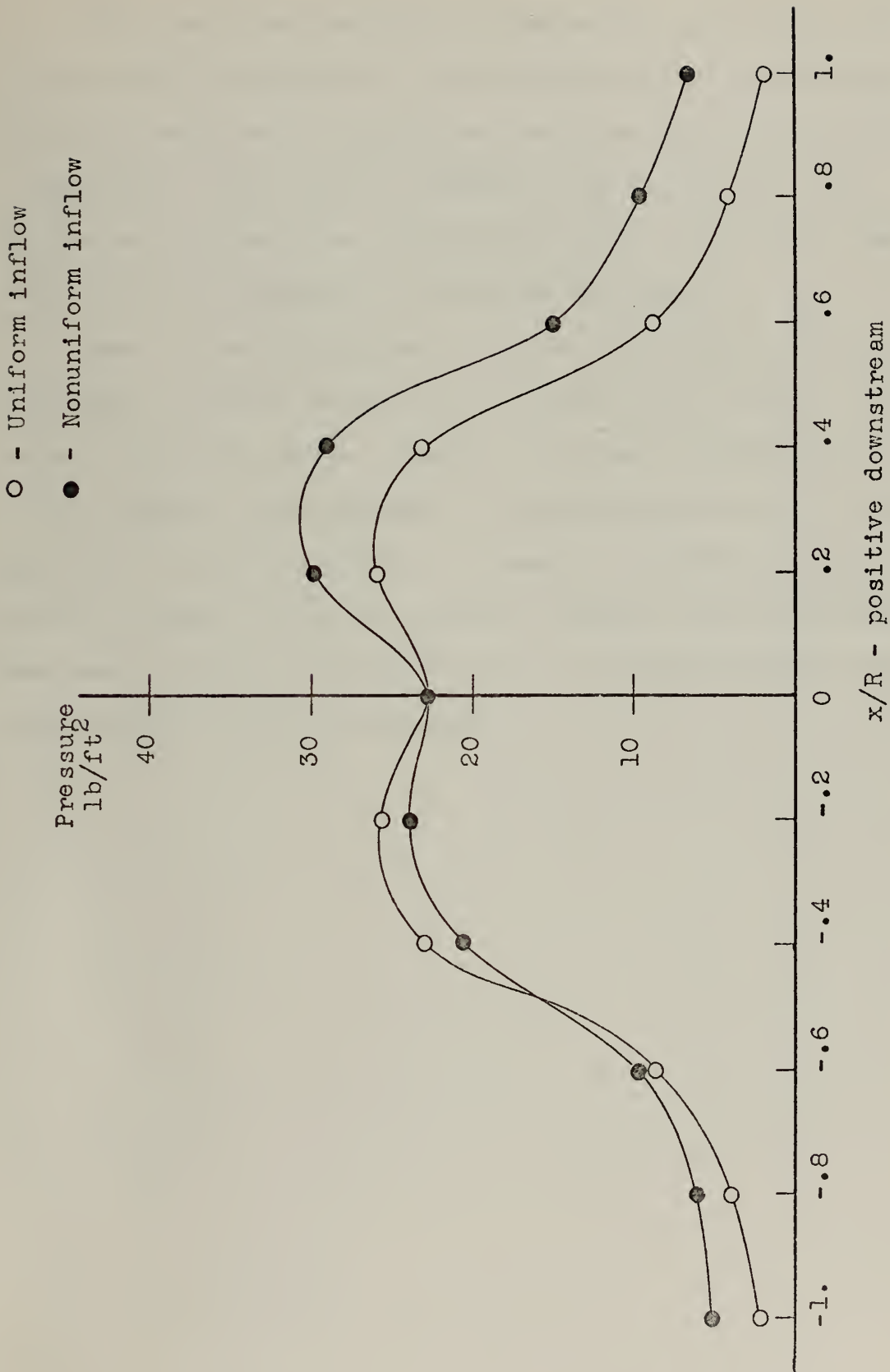
FIG. 1 - PRESSURE DISTRIBUTION FOR THE FIRST BLADE HARMONIC OF A 4 BLADE PROPPELER

The usual assumptions of an incompressible, frictionless and irrotational flow are held. It is also assumed that all the disturbances are small, which requires that the blades be thin and propeller loading small. The effects of thickness form and outline of the blades and the form of the loading distribution, both radially and over the chord are taken into account by this theory.

When this work was already under way, the Davidson Laboratory published a report by Jacobs et al. [19] which also treats the unsteady, propeller induced, pressure field using a lifting surface theory. However, their treatment is based on the solution of a Dirichlet problem for the pressure field. It seemed of interest to compare the results obtained with the two different approaches but unfortunately were were not able to obtain from D.L. the loading distribution for the propellers used in their report.

Chapter II

FORMULATION OF THE PROBLEM

It is desired to find the pressure at any point in the fluid around a ship's propeller. Assuming that the flow is incompressible, frictionless and irrotational, the problem becomes one of potential theory which in principle can be solved by finding the velocity potential and velocities induced by the propeller and substituting into the Bernoulli's equation to solve for the pressure.

1. Geometry of the Propeller

The following geometrical considerations are adopted from [1].

Two orthogonal coordinate systems -- a Cartesian (x,y,z) and a cylindrical (x,r,θ) -- are associated with the propeller as represented in Fig. 2. Both systems are fixed with the propeller and the first blade is made to coincide with the y axis. All length dimensions are nondimensionalized with respect to the radius of the propeller, R. The equations relating the two coordinate systems are:

$$y = r\cos\theta \qquad r = (y^2 + z^2)^{\frac{1}{2}}$$
$$z = r\sin\theta \qquad \theta = \tan^{-1}(z/y) \tag{1}$$

In order to relate corresponding points on each of the K blades, we define δ_k as the θ coordinate of the point at the tip of the k'th blade. For symmetrically arranged blades it is

$$\delta_k = \frac{2\pi(k-1)}{K} \qquad k = 1,2,\ldots,K \tag{2}$$

PERSPECTIVE VIEW

EXPANDED VIEW
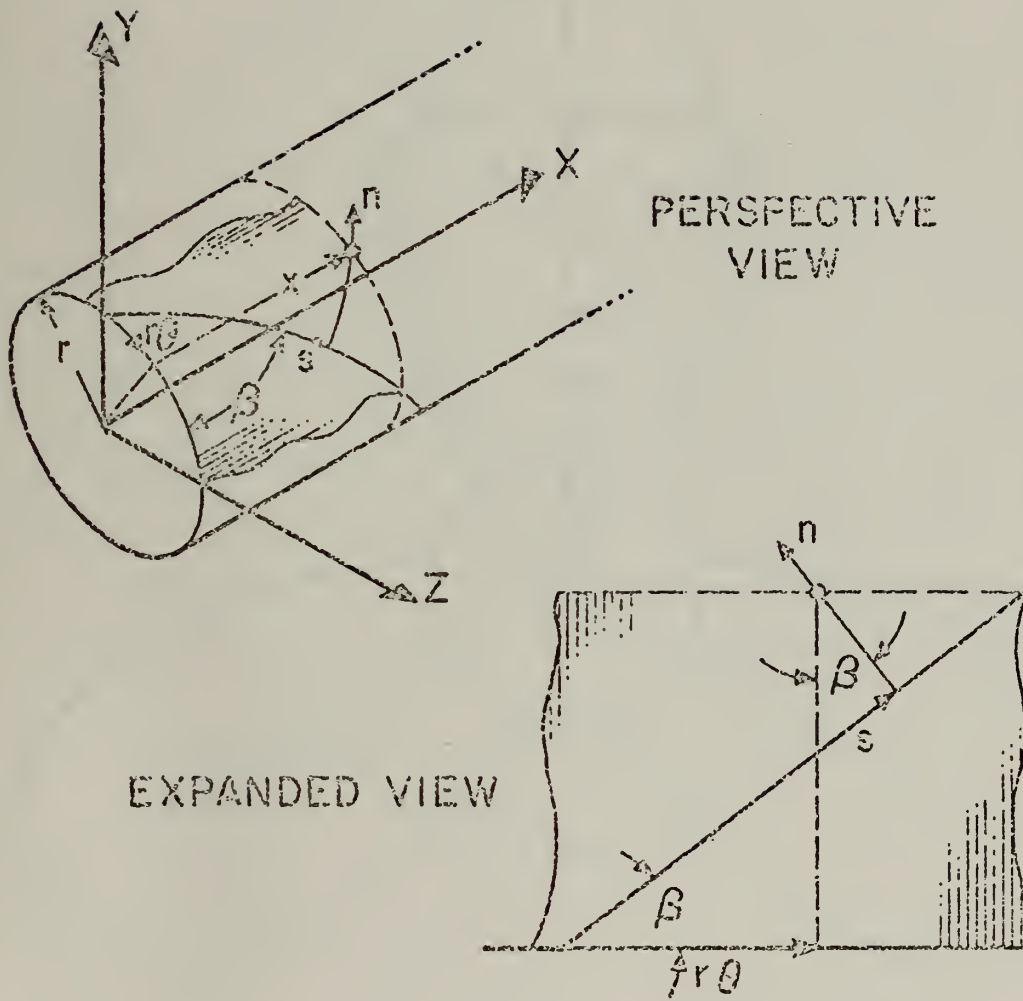
FIG. 2 - COORDINATE SYSTEMS
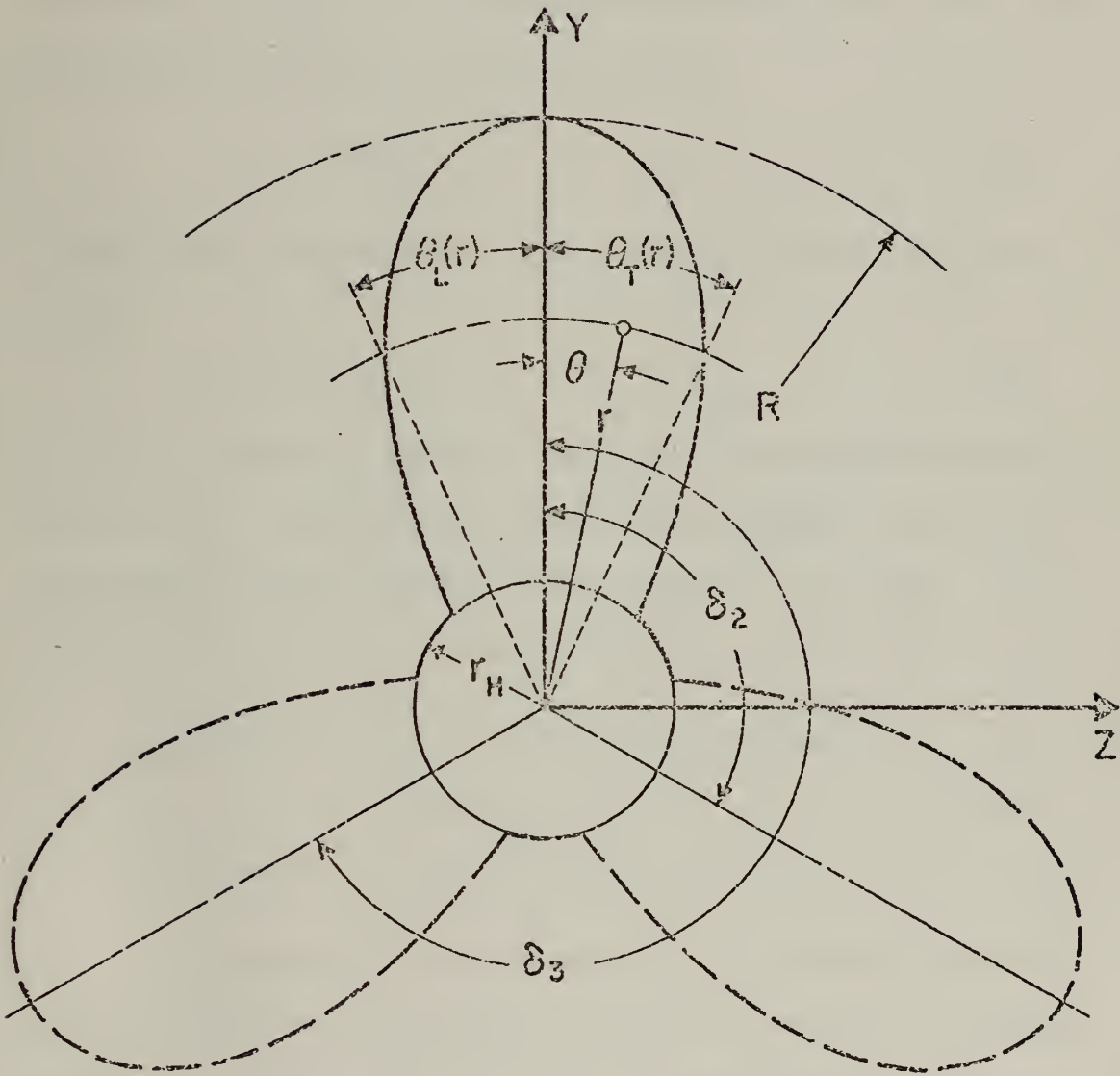
FIG. 3 - PROJECTED BLADE OUTLINE

This is illustrated in Fig. 3 which also shows the projected blade outline, defined by the angular coordinates $\theta_L(r)$ and $\theta_T(r)$ of the leading and trailing edges, respectively.

The geometry of the flow past a blade is schematically represented in Fig. 4. It is seen that the oncoming flow $V_o(r)$ forms an angle β with the yz plane, and we define

$$\lambda(r) = r \tan\beta(r) \tag{3}$$

as the "advance coefficient". The streamlines are helices with pitch

$$P(r) = 2\pi \lambda(r) \quad . \tag{4}$$

It is useful to define an orthogonal curvilinear coordinate system (s,r,n) associated with the helical surfaces swept out by the undisturbed flow past the radial lines $\{x = 0, \theta = \delta_k\}$. This system, shown in Fig. 2, has unit vectors:

$$\bar{u}_s = \bar{i} \sin\beta - \sin(\theta + \delta_k)\cos\beta + \bar{k} \cos(\theta + \delta_k)\cos\beta$$

$$\bar{u}_r = \cos(\theta + \delta_k) + \bar{k} \sin(\theta + \delta_k) \tag{5}$$

$$\bar{u}_n = \bar{i} \cos\beta + \sin(\theta + \delta_k)\sin\beta - \bar{k} \cos(\theta + \delta_k)\sin\beta$$

It is assumed that the blades lie on those helical surfaces. This assumption is in accordance with the linear theory for lightly loaded propellers, however, it does not impose any limitation to the possibility of including nonlinear refinements by suitably modifying the advance angle [1].

NO ORDER SLIPS INVOLVED
IN TECHNICAL PROCESSING
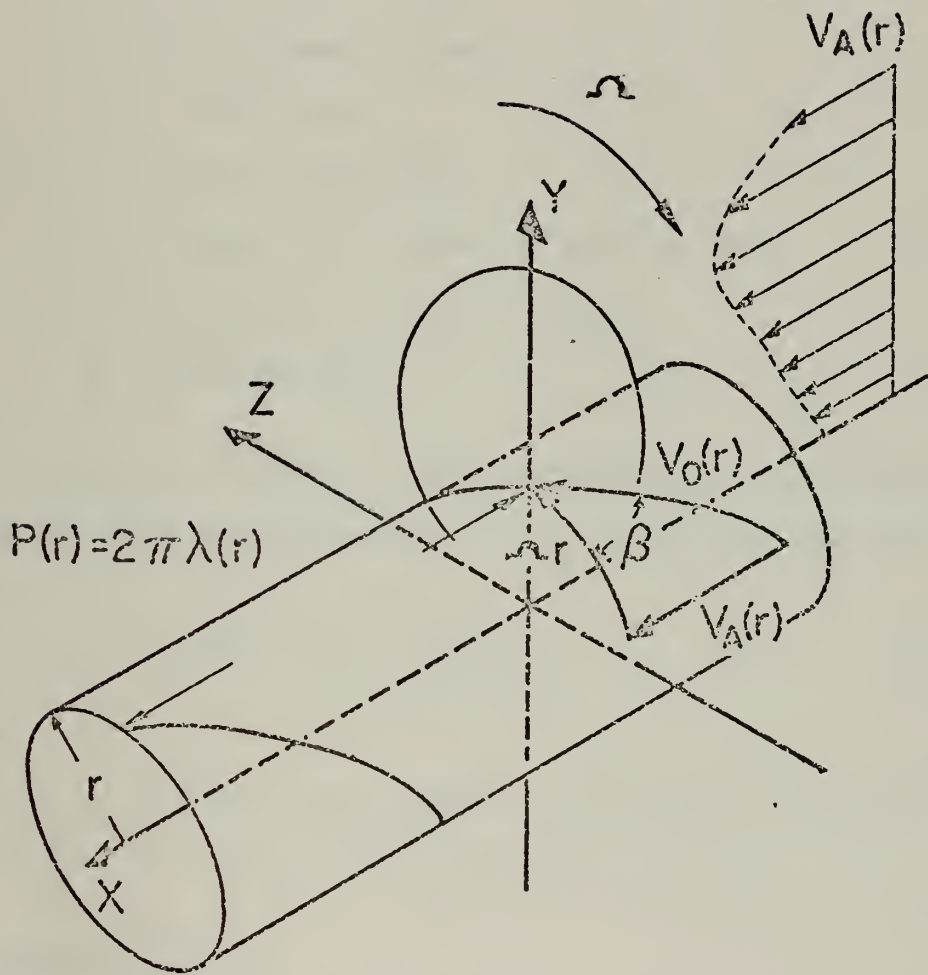
FIG. 4 - APROACH FLOW VELOCITY DIAGRAM

2. Expression for the Pressure

The Bernoulli's equation for unsteady flow is

$$p = \rho_f \frac{\partial \Phi}{\partial t} + \tfrac{1}{2} \rho_f (V_A^2 - v^2)$$

where

p = hydrodynamic pressure

ρ_f = fluid density

Φ = velocity potential

V_A = speed of free stream or speed of advance

V = resultant velocity at a point

t = time variable.

Changing to a frame of reference moving with the propeller blades and after linearization the above equation becomes [11]

$$p = \rho_f \frac{\partial \Phi}{\partial t} + \rho_f u_a V_A + \rho_f \Omega r\, u_t \qquad (6)$$

where

u_a, u_t = axial and tangential disturbance velocities

Ω = angular velocity of the propeller.

3. Induced Velocities

In order to find the velocities induced by the propeller, we make use of the vortex representation described, for instance, in [1] and [2]. The following is an adaptation to the unsteady case of the relations derived in [1].

The inflow velocity and verticity strength are expressed as complex Fourier series of the angular position of the rotating co-ordinate system with respect to a set of axes fixed in the ship,

$$V_o(\rho,\varphi t) = \bar{V}_o(\rho) \cdot e^{iN(\Omega t-\varphi)}$$

$$\gamma(\rho,\varphi,t) = \bar{\gamma}(\rho,\varphi) \cdot e^{iN\Omega t}$$

where

V_o = relative flow velocity past the blade section

γ = vorticity strength, in general

N = harmonic number

Ω = angular velocity of the propeller

(i) Velocity Induced by Source Distribution

The velocity induced at a point (x,r,θ) by sources distributed over K blades is

$$u_a^{(s)}(x,r,\theta,t) = \sum_{k=1}^{K} \frac{e^{iN(\Omega t-\delta_k)}}{4\pi} \int_{r_h}^{1} \int_{\theta_L}^{\theta_T} \bar{V}_o(\rho) \cdot$$

$$\cdot e^{-iN\varphi} \cdot \frac{\partial \tau}{\partial s} \cdot \frac{[x - \lambda(\rho)\cdot\varphi]\cdot[\rho^2+ \lambda^2(\rho)]^{\frac{1}{2}}}{D^3} \, d\varphi \, d\rho \quad (7)$$

$$u^{(s)}(x,r,\theta,t) = \sum_{k=1}^{K} \frac{-e^{iN(\Omega t-\delta_k)}}{4\pi} \int_{r_h}^{1} \int_{\theta_L}^{\theta_T} \bar{V}_o(\rho)$$

$$\cdot e^{iN\varphi} \cdot \frac{\partial \tau}{\partial s} \cdot \frac{\rho \sin(\varphi+ \delta_k - \theta)\cdot[\rho^2+ \lambda^2(\rho)]^{\frac{1}{2}}}{D^3} \, d\varphi \, d\rho \quad (8)$$

where

$$D = [(x - \lambda(\rho) \cdot \varphi)^2 + r^2 + \rho^2 - 2r\rho \cos(\varphi + \delta_k - \theta)]^{\frac{1}{2}}$$

τ = blade thickness

The superscript s denotes a source velocity.

(ii) <u>Velocity Induced by Vortex Distribution</u>

We separate the components of the induced velocities due to the bound vorticity in the blade (superscript b), radial vorticity in the wave (sup. r), streamwise vorticity in the blade (sup. f) and streamwise vorticity in the wake (sup. w).

$$u_a^{(b)}(x,r,\theta,t) = \sum_{k=1}^{K} \frac{-e^{iN(\Omega t - \delta_k)}}{4\pi} \int_{r_h}^{1} \int_{\theta_L}^{\theta_T} \bar{\gamma}_b(\rho,\varphi) \cdot$$

$$\cdot \frac{r[\rho^2 + \lambda^2(\rho)]^{\frac{1}{2}} \sin(\varphi + \delta_k - \theta)}{D^3} \, d\varphi \, d\rho \tag{9}$$

$$u_t^{(b)}(x,r,\theta,t) = \sum_{k=1}^{K} \frac{-e^{iN(\Omega t \delta_k)}}{4\pi} \int_{r_h}^{1} \int_{\theta_L}^{\theta_T} \bar{\gamma}_b(\rho,\varphi) \cdot$$

$$\cdot \frac{(x - \lambda(\rho)\varphi[\rho^2 + \lambda^2(\rho)]^{\frac{1}{2}} \cos(\varphi + \delta_k - \theta)}{D^3} \, d\varphi \, d\rho \tag{10}$$

$$u_a^{(r)}(x,r,\theta,t) = \sum_{k=1}^{K} \frac{-e^{iN(\Omega t + \theta_T - \delta_k)}}{4\pi} \int_{r_h}^{1} \int_{\theta_T}^{\infty} \bar{\gamma}_r(\rho) - \rho^{-iN\varphi} \cdot$$

$$\cdot \frac{r[\rho^2 + \lambda^2(\rho)]^{\frac{1}{2}} \sin(\varphi + \delta_k - \theta)}{D^3} \, d\varphi \, d\rho \tag{11}$$

$$u_t^{(r)}(x,r,\theta,t) = \sum_{k=1}^{K} \frac{-e^{iN(\Omega t + \theta_T - \delta_k)}}{4\pi} \int_{r_h}^{1} \int_{\theta_T}^{\infty} \bar{r}_r(\rho) \cdot \rho^{-iN\varphi} \cdot$$

$$\cdot \frac{(x - \lambda(\rho)\varphi)[\rho^2 + \lambda^2(\varphi)]^{\frac{1}{2}} \cos(\varphi + \delta_k - \theta)}{D^3} \, d\varphi \, d\rho \qquad (12)$$

$$u_a^{(f)}(x,r,\theta,t) = \sum_{k=1}^{K} \frac{e^{iN(\Omega t - \delta_k)}}{4\pi} \int_{r_h}^{1} \int_{\theta_L}^{\theta_T} \bar{r}_f(\rho,\varphi) \cdot$$

$$\cdot \frac{[\rho^2 - \rho r \cos(\varphi + \delta_k - \theta)]}{D^3} \, d\varphi \, d\rho \qquad (13)$$

$$u_t^{(f)}(x,r,\theta,t) = \sum_{k=1}^{K} \frac{e^{iN(\Omega t - \delta_k)}}{4\pi} \int_{r_h}^{1} \int_{\theta_L}^{\theta_T} \bar{r}_f(\rho,\varphi) \cdot$$

$$\cdot \left\{ \frac{\lambda(\rho)[r - \rho \cos(\varphi + \delta_k - \theta)]}{D^3} + \right.$$

$$\left. + \frac{\rho[x - \lambda(\rho)\varphi] \sin(\varphi + \delta_k - \theta)}{D^3} \right\} \, d\varphi \, d\rho \qquad (14)$$

$$u_a^{(w)}(x,r,\theta,t) = \sum_{k=1}^{K} \frac{e^{iN(\Omega t + \theta_T - \delta_k)}}{4\pi} \int_{r_h}^{1} \int_{\theta_T}^{\infty} \bar{r}_w(\rho) \cdot \rho^{-iN\varphi} \cdot$$

$$\cdot \frac{[\rho^2 - \rho r \cos(\varphi + \delta_k - \theta)]}{D^3} \, d\varphi \, d\rho \qquad (15)$$

$$u_t^{(w)}(x,r,\theta,t) = \sum_{k=1}^{K} \frac{e^{iN(\Omega t + \theta_T - \delta_k)}}{4\pi} \int_{r_h}^{1} \int_{\theta_T}^{\infty} \bar{r}_w(\rho) \cdot \rho^{-iN\varphi} \cdot$$

$$\cdot \left\{ \frac{\lambda(\rho)[r - \rho \cos(\varphi + \delta_k - \theta)}{D^3} + \frac{\rho[x - \lambda(\rho)\varphi]\sin(\varphi + \delta_k - \theta)}{D^3} \right\} \, d\varphi \, d\rho$$

$$(16)$$

where

$\bar{\gamma}_b(\rho,\varphi)$ = complex amplitude of the bound vorticity

$\bar{\gamma}_r(\rho)$ = complex amplitude of the radical vorticity

in the wake

$\bar{\gamma}_f(\rho,\varphi)$ = complex amplitude of the streamwise vorticity

in the blade

$\bar{\gamma}_w(\rho)$ = complex amplitude of the streamwise vorticity

in the wake.

3. Velocity Potential

As before we separate the effects due to source and vortex

distributions.

(i) Velocity Potential due to Source Distribution

The velocity potential at a point due to a source of unit

strength located at a distance, d, is given by [16]

$$\Phi = - \frac{1}{4\pi d}$$

Multiplying by the source strength, integrating over the first

blade and summing over the K blades gives:

$$\Phi^{(s)}(x,r,\theta,t) = \sum_{k=1}^{K} \frac{-e^{iN(\Omega t - \delta_k)}}{4\pi} \int_{r_h}^{1} \int_{\theta_L}^{\theta_T} \bar{V}_o(\rho) \cdot \rho^{-iN\varphi} \cdot \frac{\partial \tau}{\partial s} \cdot$$

$$\cdot \frac{[\rho^2 + \lambda^2(\rho)]^{\frac{1}{2}}}{D} \, d\varphi \, d\rho \tag{17}$$

(ii) Velocity Potential due to Vortex Distribution

Instead of trying to find an exact expression for the velocity potential, which would be rather cumbersome, we make use of the fact that the unsteady effects become important only at a distance from the propeller and that a reentrant vortex is, in a sense, equivalent to a uniform distribution of double sources over any surface bounded by it. It is shown in Appendix A that if we substitute a reentrant vortex by an equivalent concentrated doublet, the error in the value of the velocity potential decreases rapidly with distance.

In this way we can compute the velocity potential by summing a set of discrete values given by expressions of the form (see Appendix A)

$$\Phi = \frac{S \cos \Psi}{4\pi D^2}$$

where

S = strength of the concentrated doublet

Ψ = angle between the doublet axis and the line from the doublet to the field point.

The value of S will be found later and $\cos \Psi$ is easily computed from

$$\cos \Psi = \frac{\bar{n} \cdot \bar{D}}{|\bar{n}| \cdot \bar{D}}$$

where

$\bar{n}$ = vector direction of the double axis

$\bar{D} = [x - \lambda(\rho)\varphi]\bar{i} + [r \cos\theta - \rho \cos(\varphi + \delta_k)]\bar{j} +$
$\qquad + [r \sin\theta - \rho \sin(\varphi + \delta_k)]\bar{k}$

Using (5) to obtain $\bar{n}$, it follows that

$$\cos \Psi = \frac{[x - \lambda(\rho)\varphi]\cos\beta(\rho) + r \sin\beta(\rho)\cos(\varphi + \delta_k - \theta)}{D} \tag{19}$$

4. The Loading Modes

For the purposes of this work it is assumed that the distribution of the loading on the propeller blades has already been determined by any of the known methods (examples [2], [3], [7], [12] and [15]) which solve the unsteady lifting surface problem of a propeller operating in a wake. The usual procedure in these methods is to assume that the loading may be expressed in separable form as the product of a function of the spanwise coordinates and a function of the chordwise coordinates. In selecting these functions, one makes use of the known results of the theory for incompressible flow in two dimensions and of the lifting line theory for the higher aspect ratio wings. This leads to functions of the type

$$\Delta p = \sum_{n=0}^{\infty} F_n(s) \times G_n(r)$$

where

Δp = loading per unit area

$F_n(s)$ = chordwise function

$G_n(r)$ = spanwise function.

Two dimensional airfoil theory suggests that we choose F_n of the form, [5]

$$F_n(\xi) = \left[\frac{1 - \xi}{1 + \xi} \right]^{\frac{1}{2}} + \sin[n(\cos^1 \xi)]$$

where

$$\xi = \frac{2(s - s_{LE})}{\ell} - 1$$

ℓ = chord length

Introducing a new coordinate $\hat{\theta}$ defined by

$$s = \frac{s + s_{LE}}{2} - \frac{\ell}{2} \cos\hat{\theta} \qquad 0 \leq \hat{\theta} \leq \pi$$

F_n becomes

$$F_n(\hat{\theta}) = \cotan \frac{\hat{\theta}}{2} + \cos(n\pi)\sin(n\hat{\theta})$$

The spanwise function $G_n(r)$ is either determined directly with the aid of a specially selected interpolation function [5] or expressed in the form

$$G_n(r) = \sum_m A_{nm} H_m(r)$$

and then determined by the solution of the integral equation resulting from the formulation of the lifting surface problem. In order to obtain a numerical solution $G_n(r)$ is usually approximated by a stepwise distribution.

The loading then will be of the form

$$\Delta p(r,\hat{\theta}) = L_o(r) \cot \frac{\hat{\theta}}{2} + \sum_{n=1}^{\infty} L_n(r) \sin(n\hat{\theta}) \qquad (20)$$

where L_o and L_n are stepwise functions of the radius. This is called the Birnbaum distribution.

When the loading is expressed in terms of the bound vorticity, it is necessary to add an extra term to the Birnbaum modes in order

to satisfy the Kutta condition at the trailing edge [13]. In this case it becomes

$$\gamma_b(r,\hat{\theta}) = A_o(r) \cot\frac{\hat{\theta}}{2} + \sum_{n=1}^{\infty} A_n(r) \sin(n\hat{\theta}) + f(r,\hat{\theta}) \tag{21}$$

where the Kutta condition requires that

$$f(r,\pi) = \gamma_b(r,\pi) = -ik_n\Gamma \tag{22}$$

where

$$k_n = \frac{N\,\Omega\,\ell(r)}{2V_o(r)}$$

Γ = chordwise integration of γ_b

According to Brown [3] a convenient choice for $f(r,\hat{\theta})$ is

$$f(r,\hat{\theta}) = -ik_n\Gamma \times \frac{1 - \cos\hat{\theta}}{2}$$

After substituting into (21) and integrating over the chord, it follows that

$$f(r,\hat{\theta}) = -\pi \times \frac{ik_n}{1 + ik_n} \times (A_o + \tfrac{1}{2}A_1) \times \frac{1 - \cos\hat{\theta}}{2} \tag{23}$$

It must be noted that there is no correspondence (except for the zeroth harmonic) between the coefficients of (20) and (21). However, when the loading is given in terms of pressure distribution one can always find the corresponding vorticity distribution from the solution of the following Volterra equation of the second kind [14]

$$\frac{\Delta p(r,s,t)}{\rho_f} = \frac{\partial}{\partial t}\int_{S_{\ell}}^{S}\gamma_b(r,s,t)ds + V_o(r)\,\gamma_b(r,s,t) \tag{24}$$

in terms of $\hat{\theta}$ the above expression becomes

$$\gamma_b(r,\hat{\theta}) = \frac{\Delta p(r,\hat{\theta})}{\rho_f V_o(r)} - ik_n(r) \int_0^{\hat{\theta}} \sin\hat{\theta} \; \gamma_b(r,\hat{\theta}) \; d\hat{\theta} \tag{25}$$

5. The Vorticity Relations

The pulsating bound vorticity is expressed in the form

$$\gamma_b(\rho,\varphi,k,t) = \hat{\bar{\gamma}}_b(\rho,\varphi) \; e^{iN(\Omega t - \delta_k)} \tag{26}$$

All the other components of the vorticity can be expressed in terms of $\bar{\gamma}_b$, as required to preserve continuity of vorticity (see [1] and [2] for detailed derivation)

$$\gamma_f(\rho,\varphi,k,t) = \bar{\gamma}_f(\rho,\varphi) \; e^{iN(\Omega t - \delta_k)} \tag{27a}$$

$$\bar{\gamma}_f(\rho,\varphi) = - \int_{\theta_L}^{\varphi} \frac{\partial}{\partial\rho} \{\bar{\gamma}_b(\rho,\varphi) \cdot [\rho^2 + \lambda^2(\rho)]^{\frac{1}{2}}\} d\varphi \tag{27b}$$

$$\gamma_w(\rho,\varphi,k,t) = \bar{\gamma}_w(\rho) \; e^{iN[\Omega t - (\varphi - \theta_T) - \delta_k]} \tag{28a}$$

$$\bar{\gamma}_w(\rho) = - \frac{\partial \bar{\Gamma}(\rho)}{\partial\rho} \tag{28b}$$

$$\gamma_r(\rho,\varphi,k,t) = \bar{\gamma}_r(\rho) \; e^{iN[\Omega t - (\varphi - \theta_T) - \delta_k]} \tag{29a}$$

$$\bar{\gamma}_r(\rho) = - \frac{iN \bar{\Gamma}(\rho)}{[\rho^2 + \lambda^2(\rho)]^{\frac{1}{2}}} \tag{29b}$$

where

$$\bar{\Gamma}(\rho) = \int_{\theta_L}^{\theta_T} \bar{\gamma}_b(\rho,\varphi) \cdot [\rho^2 + \lambda^2(\rho)]^{\frac{1}{2}} \; d\varphi \tag{30}$$

Notice that γ_w and γ_r (streamwise and radial vorticity in the wake)

are expressed as the product of a complex amplitude at the trailing

edge and a sinusoidal time and distance variation along the helical

surfaces in the streamwise direction. This form had already been

implied in eqs. (6), (7), (10) and (11).

Chapter III

NUMERICAL SOLUTION

The following is an outline of the computational model used to solve the equations derived in the previous chapter.

The blades and wake are divided into chordwise panels and these panels are subdivided by radial grid lines as shown in Fig. 6. The scheme for dividing the span is shown below.
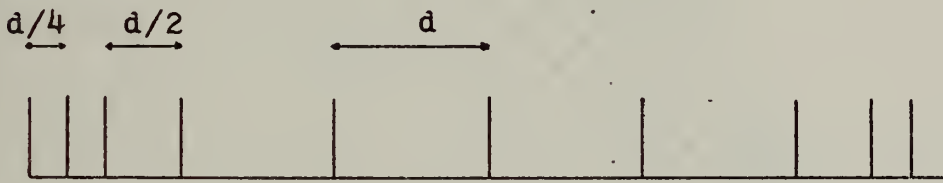
FIG. 5 - SPAN SUBDIVISION FOR NUMERICAL SOLUTION

The interval is first divided into MN equal spaces. The intervals at each end are then subdivided into half and quarter spaces as shown. The result is MT = MN + 4 chordwise panels. The chord length, pitch, rake, bound circulation strength and source strength are assumed to be independent of radius within each of the panels, with values matching those of the continuous functions at the mid-radius. The continuous trailing vortex sheet then becomes a set of MT + 1 concentrated trailing vortex lines at each of the panel boundaries.
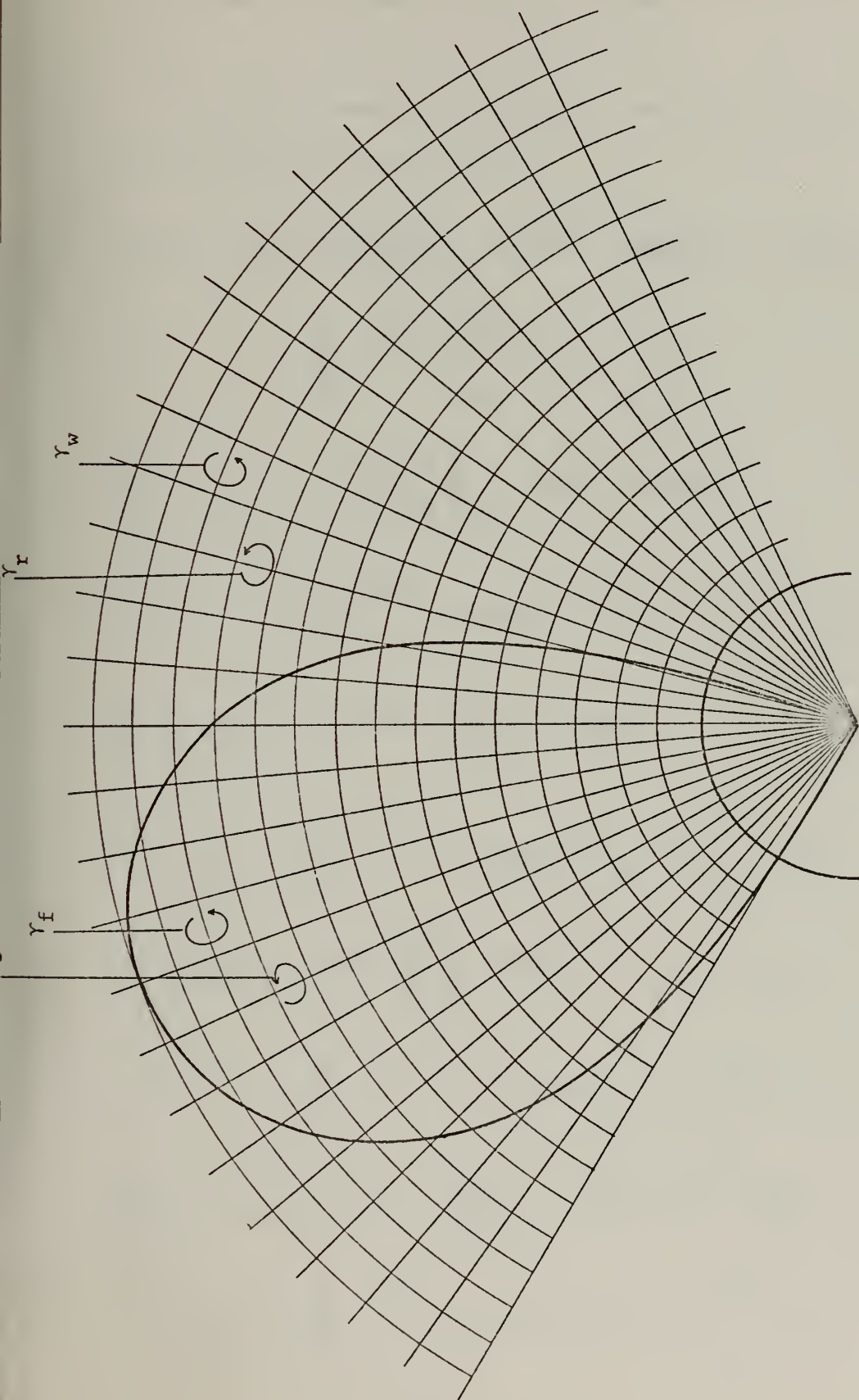
FIG. 6 - BLADE AND WAKE LATTICE FOR NUMERICAL SOLUTION

The bound circulation in the blade and the radial circulation in the wake are assumed concentrated at each of the radial grid lines.

The above assumptions allow us to write the integrals (7) to (12) as summations, as follows:

$$
u_a^{(s)}(x,r,\theta,t) = e^{iN\Omega t} \sum_{m=1}^{MT} \sum_{i=1}^{I} e^{-iN\varphi(i)} \cdot \frac{SB(m,i)}{2} [x - \lambda(m)\cdot\varphi(i)]
$$

$$
\sum_{k=1}^{K} e^{-iN\delta_k} \int_{\rho_m}^{\rho_{m+1}} \frac{d\rho}{D^3} \tag{31}
$$

$$
u_t^{(s)}(x,r,\theta,t) = -e^{iN\Omega t} \sum_{m=1}^{MT} \sum_{i=1}^{I} e^{-iN\varphi(i)} \cdot \frac{SB(m,i)}{2}
$$

$$
\sum_{k=1}^{K} e^{-iN\delta_k} \cdot \sin(\varphi(i) + \delta_k - \theta) \cdot \int_{\rho_m}^{\rho_{m+1}} \rho \frac{d\rho}{D^3} \tag{32}
$$

$$
u_a^{(b)}(x,v,\theta,t) = -e^{iN\Omega t} \cdot r \cdot \sum_{m=1}^{MT} \sum_{i=1}^{I} \frac{GB(m,i)}{2}
$$

$$
\sum_{k=1}^{K} e^{-iN\delta_k} \cdot \sin(\varphi(i)+\delta_k - \theta) \int_{\rho_m}^{\rho_{m+1}} \frac{d\rho}{D^3} \tag{33}
$$

$$
u_t^{(b)}(x,r,\theta,t) = -e^{iN\Omega t} \sum_{m=1}^{MT} \sum_{i=1}^{I} \frac{GB(m,i)}{2} \cdot (x - \lambda(m)\cdot\varphi(i))
$$

$$
\sum_{k=1}^{K} e^{-iN\delta} \cdot \cos(\varphi(i)+\delta_k - \theta) \cdot \int_{\rho_m}^{\rho_{m+1}} \frac{d\rho}{D^3} \tag{34}
$$

$$
u_a^{(r)}(x,r,\theta,t) = -e^{iN\Omega t} \cdot r \cdot \sum_{m=1}^{MT} \sum_{i=I}^{\infty} e^{iN(\theta_T -\varphi(i))} \cdot \frac{GR(m)}{2}
$$

$$
\sum_{k=1}^{K} e^{-iN\delta_k} \cdot \sin(\varphi(i)+\delta_k - \theta) \cdot \int_{\rho_m}^{\rho_{m+1}} \frac{d\rho}{D^3} \tag{35}
$$

$$u_t^{(r)}(x,r,\theta,t) = -e^{iN\Omega t} \sum_{m=1}^{MT} \sum_{i=I}^{\infty} e^{iN(\theta_T - \varphi(i))} \cdot \frac{GR(m)}{2} \cdot (x - \lambda(m) \cdot \varphi(i))$$

$$\sum_{k=1}^{K} e^{-iN\delta_k} \cdot \cos(\varphi(i) + \delta_k - \theta) \; ; \; \int_{\rho_m}^{\rho_{m+1}} \frac{d\rho}{D^3} \tag{36}$$

where

SB(m,i) = amplitude of the equivalent source strength, concentrated at the i'th grid line in the m'th panel.

GB(m,i) = amplitude of the equivalent bound vorticity, con-centrated at the i'th grid line in the m'th panel.

GR(m) = amplitude of the radial vorticity in the wake, con-centrated at the i'th grid line in the m'th panel.

In the above equations the source and vortex strengths are non-dimensionalized with respect to $2\pi RV_s$, and the perturbation velocities are non-dimensionalized with respect to V_s.

The integrals that appear in the equations above are evaluated between the limits of integration corresponding to the boundaries of each panel and can be determined analytically as follows

$$\int_{\rho_m}^{\rho_{m+1}} \rho \frac{d\rho}{D^3} = - \left. \frac{r\rho\cos(\varphi(i) + \delta_k - \theta) + (x - \lambda(m)\cdot\varphi(i))^2 + r^2}{\{[x - \lambda(m)\varphi(i)] + r^2\sin^2(\varphi(i) + \delta_k - \theta)\}\cdot D} \right|_{\rho_m}^{\rho_{m+1}}$$

$$\int_{\rho_m}^{\rho_{m+1}} \frac{d\rho}{D^3} = \left. \frac{\rho - r\cos(\varphi(i) + \delta_k - \theta)}{[(x - \lambda(m)\varphi(i))^2 + r^2\sin^2(\varphi(i) + \delta_k - \theta)]\cdot D} \right|_{\rho_m}^{\rho_{m+1}}$$

The contribution from the trailing vortices -- eqs. (13)-(16)--raises the problem of streamwise integrals that cannot be evaluated

analytically. It was found by Kerwin [18] that for the zeroth

harmonic a simple trapezoidal integration is as efficient as more

sophisticated quadrature formulas, except for nearby elements. In

order to investigate the application of this argument to other har-

monics, we carried out the integration for a single trailing vortex

line located at 0.75R, using a Gaussian quadrature and a trapezoidal

rule. The computation of the perturbation velocities was carried

for different points around the propeller using a third harmonic of

the loading. We found that the results obtained with the two for-

mulas differ in all cases by less than 2 percent. However, due to

the pulsating character of the wake vorticity it is necessary to keep

the intervals of integration small compared with the wavelength of

the perturbation. This results in a very large number of computations

for each fortex line (about 1100 for a field point in the plane of

the propeller). A better alternative was found by substituting the

infinite integrals by an infinite series of finite integrals and then

applying the Euler transformation to speed up the convergency of the

series. Basicly the method works as follows:

Given an infinite integral of the type

$$I = \int_0^\infty e^{iNx} \cdot f(x) \ dx$$

it is transformed into the infinite series

$$I = \sum_{k=0}^\infty \int_{k\pi/N}^{(k+1)\pi/N} e^{iNx} \cdot f(x) \ dx =$$

$$= \sum_{k=0}^\infty (-1)^k \int_0^{\pi/N} e^{iNt} \cdot f(t + k \frac{\pi}{N}) \ dt$$

Now, applying the Euler Transformation [21], the above series
becomes

$$I = \sum_{k=0}^{\infty} \frac{(-1)^k \Delta^k a_o}{2^{k+1}} \; , \qquad \Delta^k a_o = \sum_{m=0}^{k} (-1)^m \binom{k}{m} a_{k-m}$$

$$a_k = \int_0^{\pi/N} e^{iNt} \cdot f(t + k\,\pi/N)\,dt$$

Sample computations done with this method showed good convergence
with a fairly reduced number of terms. Also, it was found that a
5-point Gaussian quadrature was adequate for the computation of the
terms of the series.

When the above transformations are applied to eqs. (15) and
(16), we obtain

$$u_a^{(w)}(x,r,\theta,t) = e^{iN\Omega t} \sum_{m=1}^{MT+1} e^{iN\theta_T(m)} \cdot \frac{TL(m)}{2} \sum_{k=1}^{K} e^{-iN\delta_k} \cdot$$

$$\cdot \sum_{J=0}^{\infty} \frac{(-1)^J \cdot \Delta^J a_o}{2^{J+1}} \; , \tag{37}$$

$$a_J = \int_0^{\pi/N} e^{-iN(\xi+\theta_T)} \cdot FWA(\xi + \theta_T + k\,\pi/N)\,d\xi$$

$$u_t^{(w)}(x,r,\theta,t) = e^{iN\Omega t} \cdot \sum_{m=1}^{MT+1} e^{iN\theta_T(m)} \cdot \frac{TL(m)}{2} \sum_{k=1}^{K} e^{-iN\delta_k}$$

$$\cdot \sum_{J=1}^{\infty} \frac{(-1)^J \cdot \Delta^J a_o}{2^{J+1}} \; , \tag{38}$$

$$a_J = \int_0^{\pi/N} e^{-iN(\xi+\theta_T)} \cdot FWT(\xi + \theta_T + k\,\pi/N)\,d\xi$$

where

$\text{TL}(m)$ = amplitude of the m'th trailing vortex, on the wake

$$\text{FWA}(\varphi) = \frac{\rho_m[\rho_m - r\,\cos(\varphi + \delta_k - \theta)]}{D^3}$$

$$\text{FWT}(\varphi) = \{-\rho_m[\lambda(m)\cos(\varphi + \delta_k - \theta) - (x - \lambda(m)\cdot\varphi)\sin(\varphi + \delta_k - \theta)] + r\cdot\lambda(m)\}/D^3$$

It is clear that eqs. (37) and (38) cannot be applied to the zeroth harmonic of the loading because the upper limit of the integrals would go to infinity. Instead, we will use the trapezoidal rule which was found appropriate for this case, as mentioned before. Using a trapezoidal rule, eqs. (15) and (16) become

$$u_a^{(w)}(x,r,\theta,t) = e^{iN\Omega t} \sum_{m=1}^{MT+1} \sum_{i=I}^{\infty} e^{iN(\theta_T - \varphi(i))} \cdot \frac{\text{TL}(m,i) + \text{TL}(m,i-1)}{4}$$

$$\rho_m \cdot \sum_{k=1}^{K} e^{-iN\delta_k} \frac{\rho_m - r\,\cos(\varphi(i) + \delta_k - \theta)}{D^3} \qquad (39)$$

$$u_t^{(w)}(x,r,\theta,t) = e^{iN\Omega t} \cdot \sum_{m=1}^{MT+1} \sum_{i=I}^{\infty} e^{iN(\theta_T - \varphi(i))} \cdot \frac{\text{TL}(m,i) + \text{TL}(m,i-1)}{4}$$

$$\sum_{k=1}^{K} e^{-iN\delta_k} \{-\rho_m[\lambda(m)\cos(\varphi(i) + \delta_k - \theta) -$$

$$(x - \lambda(m)\varphi(i))\cdot\sin(\varphi(i) + \delta_k - \theta)]\ r\ \lambda(m)\}/D^3$$

$$\qquad (40)$$

The contribution from the trailing vortices on the blade -- eqs. (13) and (14) -- are computed using a trapezoidal integration, for all the harmonics,

$$u_a^{(f)}(x,r,\theta,t) = e^{iN\Omega t} \sum_{m=1}^{MT+1} \sum_{i=1}^{I} \frac{GT(m,i) + GT(m,i-1)}{4} \cdot$$

$$\cdot \rho_m \sum_{k=1}^{K} e^{-iN\delta_k} \frac{\rho_m - r \cos(\varphi(i) + \delta_k - \theta)}{D^3} \tag{41}$$

$$u_t^{(f)}(x,r,\theta,t) = e^{iN\Omega t} \sum_{m=1}^{MT+1} \sum_{i=1}^{I} \frac{GT(m,i) + GT(m,i-1)}{4} \cdot$$

$$\cdot \sum_{k=1}^{K} e^{-iN\delta_k} \{-\rho_m[\lambda(m)\cos(\varphi(i) + \delta_k - \theta) -$$

$$(x - \lambda(m)\varphi(i) \cdot \sin(\varphi(i) + \delta_k - \theta)] + r \ \lambda(m)\}/D^3 \tag{42}$$

where

GT(m,i) = Amplitude of the m'th trailing vortex located

on the blade, between the i'th and the i'th+1

grid lines.

The triple summations corresponding to the velocity potential

due to the source and vortex distributions -- eqs. (17) and (18)-- are

$$\Phi^{(s)}(x,r,\theta,t) = -e^{iN\Omega t} \sum_{m=1}^{MT} \sum_{i=1}^{I} e^{-iN\varphi(i)} \cdot \frac{SB(m,i)}{2} \cdot$$

$$\sum_{k=1}^{K} e^{-iN\delta_k} \cdot \int_{\rho_m}^{\rho_{m+1}} \frac{d\rho}{D} \tag{43}$$

$$\Phi_b^{(b)}(x,r,\theta,t) = -e^{iN\Omega t} \sum_{m=1}^{MT} \sum_{i=1}^{I} \frac{GP(m,i)}{2} \cdot \sum_{k=1}^{K} e^{-iN\delta_k} \cdot$$

$$\frac{(x - \lambda(m)\cdot\varphi(i))\cos \beta(m) + r \ \sin \beta(m) \ \cos(\varphi(i) + \delta_k - \theta)}{D} \tag{44}$$

$$\Phi_w^{(b)}(x,r,\theta,t) = -e^{iN\Omega t} \sum_{m=1}^{MT} \sum_{i=1}^{\infty} \frac{GL(m,i)}{2} \sum_{k=1}^{K} e^{-iN\delta_k}$$

$$\frac{(x - \lambda(m)\cdot\varphi(i))\cos\beta(m) + r\sin\beta(m)\cos(\varphi(i)+\delta_k - \theta)}{D}$$

(45)

where

$\Phi_b^{(b)}$ = velocity potential due to the vorticity in the blade.

$\Phi_w^{(b)}$ = velocity potential due to the vorticity in the wake.

GP(m,i) = amplitude of the concentrate vortex equivalent to

GB(m,i).

GL(m,i) = amplitude of the concentrate vortex equivalent to

GR(m,i).

The integral appearing in eq. (43) is evaluated analytically

$$\int_{\rho_m}^{\rho_{m+1}} \frac{d\rho}{D} = \ell n \left| 2(D + \rho - r\cos(\varphi(i)+\delta_k - \theta)) \right| \Big|_{\rho_m}^{\rho_{m+1}}$$

The value of the bound circulation is obtained either directly if the loading is expressed as in eq. (21) or after solving a Volterra equation (25) if it is expressed as in eq. (20).

The solution of the Volterra equation can be obtained using the Liouville-Neumann method of successive substitutions [20]. This gives

$$\gamma_b(r,\theta) = \frac{1}{\rho_f\cdot V_o(r)} [\Delta p(r,\hat{\theta}) - (iK_n(r) +$$

$$\sum_{k=1}^{\infty} (-1)^k \cdot \frac{(ik_n(r))^{k+1}}{K!} \cos^k\hat{\theta}\ e^{-ik_n(r)} \cdot \int_0^{\hat{\theta}} \Delta p(r,t)\sin t\, dt]$$

(46)

When the pressure loading is given in the form of Birnbaum modes

(20), the above integral is evaluated using the relations

$$\int_0^{\hat{\theta}} \cotan \frac{t}{2} \sin t \, dt = \hat{\theta} - \sin\hat{\theta}$$

$$\int_0^{\hat{\theta}} \sin nt \sin t \, dt = \frac{\hat{\theta}}{2} - \frac{1}{4} \sin(2\hat{\theta}) \,, \quad n = 1$$

$$\frac{\sin((n-1)\cdot\hat{\theta})}{2(n-1)} - \frac{\sin((n+1)\cdot\hat{\theta})}{2(n+1)} \,, \quad n \neq 1$$

Chapter IV

RESULTS

The numerical solution developed in the preceding chapter was
put into computer form; the details of the program are presented in
Appendix B. In order to test the workability of this program we
used it to compute the pressure at an upstream field point using the
NSRDC Propeller No. 4118 [22]. The design characteristics and oper-
ating conditions of this propeller are represented in Figs. 7 and 8.
We considered both the open water condition and the nonuniform wake
obtained with a screen which produces a circumferentially varying
sinusoidal wake composed only of multiplies of blade harmonics.
Unfortunately, we did not have information about the loading distri-
bution for those conditions and therefore we used an arbitrary number
of modes of the Birnbaum distribution with coefficients equal to
unit. In order to test the solution of the Volterra equation (46)
the input loading was expressed in terms of pressure distribution
rather than vorticity distribution.

We made several sample calculations in order to evaluate the
effect of changing the grid spacings and to determine how far down-
stream we needed to carry the streamwise integrations in the wake
(Table 1 shows a sample of the computer output for one of the cal-
culations). We found that for the field point considered ($x = -.8$,
$r = 1.2$, $\theta = 0$), we needed about 20 chordwise panels and had to keep
the angular grid spacing down to 2 degrees. The contribution due to

r/R=1.0
.9
.8
.7
.6
.5
.4
.3
.2

D   = 12 inches

D_{hub}= 2.4 inches
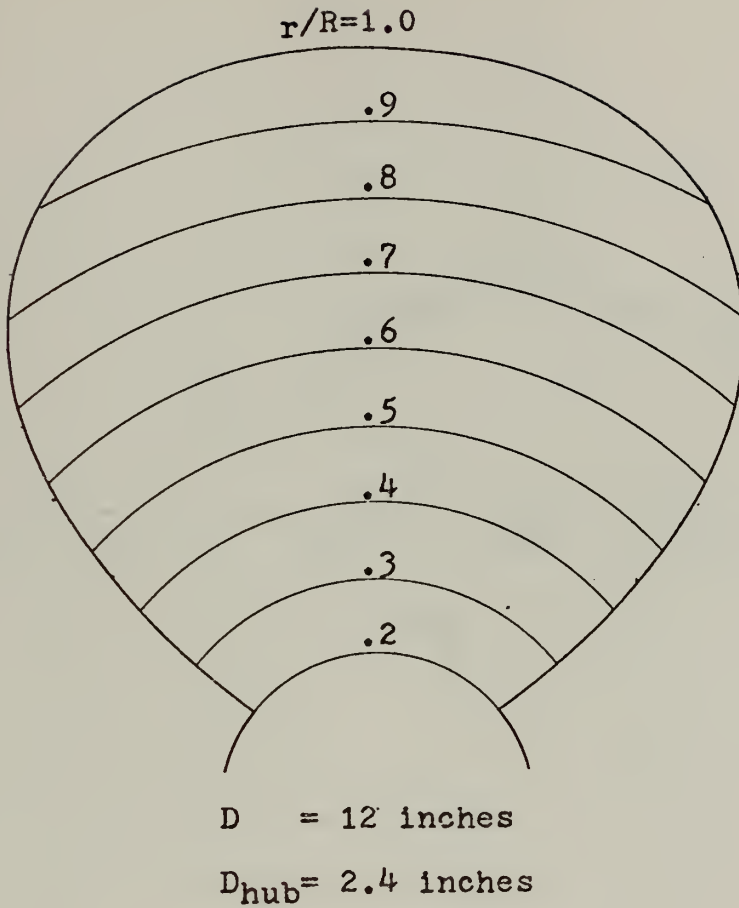
r/R	l/D	T/l	P/D
0.2	0.3200	0.1028	1.0860
0.3	0.3635	0.0776	1.0845
0.4	0.4048	0.0590	1.0823
0.5	0.4392	0.0451	1.0796
0.6	0.4610	0.0348	1.0780
0.7	0.4622	0.0271	1.0766
0.8	0.4347	0.0210	1.0750
0.9	0.3613	0.0166	1.0735
1.0	------	------	1.0700

FIG. 7 - PROPELLER 4118 DESIGN CHARACTERISTICS
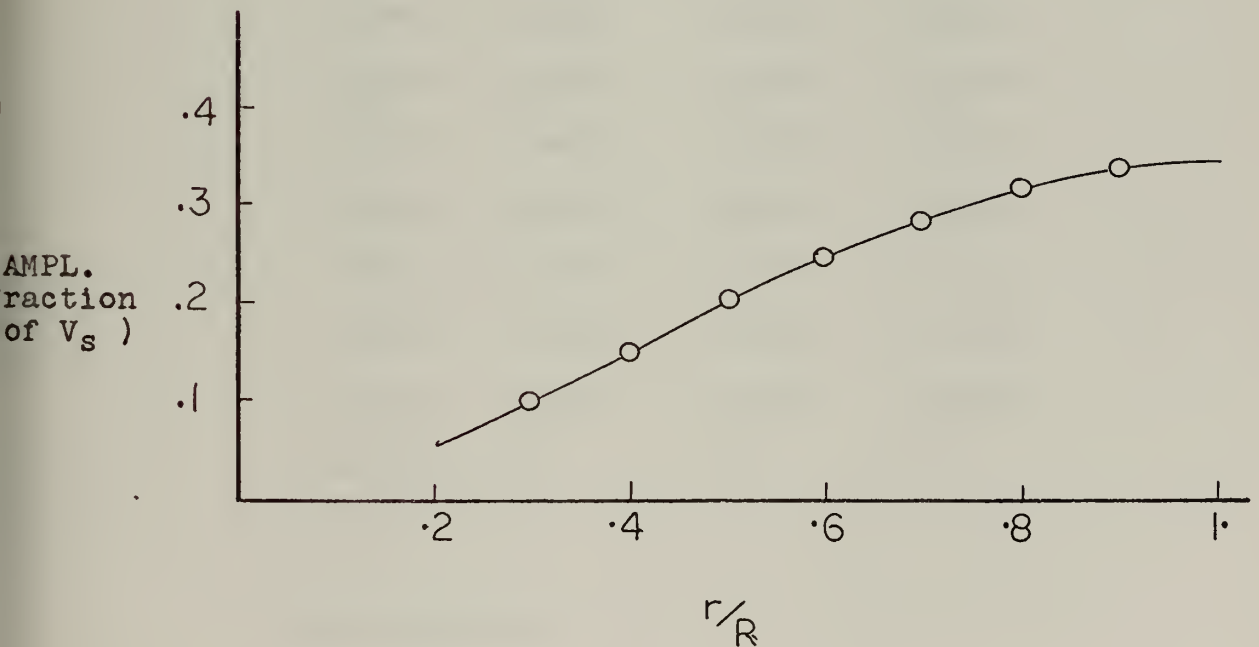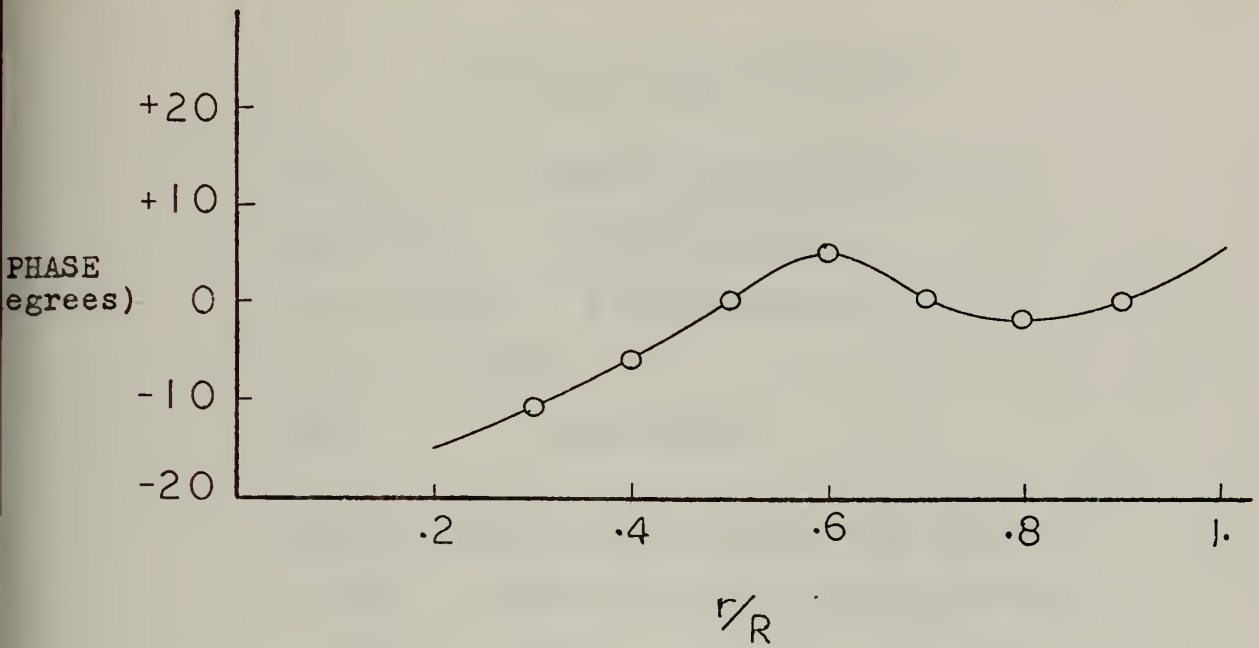
FIG. 8 - RADIAL DISTRIBUTION OF THE AMPLITUDES AND

PHASES OF THE THIRD HARMONIC OF THE

CIRCUNFERENTIAL WAKE VARIATION

******** PRESSURE FIELD AROUND A MARINE PROPELLER **`````**

PROPELLER CHARACTERISTICS

TYPE   NSRDC. PROPELLER NO.4118

DIAMETER   12.0000 INCHES

HUB DIAMETER 2.4000 INCHES

NO. OF BLADES 3

RPM   1080.0000

BLADE OUTLINE (UNITS-FRACTION OF RADIUS)

RADII	LEAD.EDGE	TRAIL.EDGE	MAX.THICK.
0.250	-0.3417	0.3417	0.0605
0.300	-0.3635	0.3635	0.0564
0.400	-0.4048	0.4048	0.0478
0.500	-0.4392	0.4392	0.0396
0.600	-0.4610	0.4610	0.0321
0.700	-0.4615	0,4615	0.0250
0.800	-0.4347	0.4347	0.0183
0.900	-0.3613	0.3613	0.0120
0.950	-0.2500	0.2500	0.0065
1.000	0.0	0.0	0.0

GRID SPACING

NO. OF CHORDWISE PANELS   20
ANGULAR CHORDWISE SPACING 0.0349066 RADIANS

TABLE 1 - SAMPLE COMPUTER OUTPUT

INFLOW CHARACTERISTICS

SYMBOLS AND UNITS

VS	SHIP SPEED, KNOTS
RADII	FRACTION OF RADIUS
XVXO	ZEROTH HARMONIC OF INFLOW / VS
TANBETA	TANGENT OF ADVANCE ANGLE
NHARM	HARMONIC NUMBER
XVXN	AMPLITUDE OF NHARM OF INFLOW / VS
XPHN	PHASE OF NHARM OF INFLOW, RADIANS

VS= 8.8780   NHARM= 3

RADII	XVXO	TANBETA	XVXN	XPHN
0.250	1.0000	1.0606	0.0800	-0.2269
0.300	1.0000	0.8838	0.1000	-0.1920
0.400	1.0000	0.6629	0.1500	-0.1047
0.500	1.0000	0.5303	0.2000	0.0
0.600	1.0000	0.4419	0.2500	0.0873
0.700	1.0000	0.3788	0.2900	0.0
0.800	1.0000	0.3314	0.3200	-0.0314
0.900	1.0000	0.2946	0.3400	0.0
0.950	1.0000	0.2791	0.3450	0.0436

TABLE 1 (cont.)

LOADING DISTRIBUTION

(VORTICITY MODES)

RADII	MODE	COEF.	
		REAL	IMAG.
0.250	1	0.014860	0.014860
0.250	2	0.014860	0.014860
0.250	3	0.014860	0.014860
0.300	1	0.014860	0.014860
0.300	2	0.014860	0.014860
0.300	3	0.014860	0.014860
0.400	1	0.014860	0.014860
0.400	2	0.014860	0.014860
0.400	3	0.014860	0.014860
0.500	1	0.014860	0.014860
0.500	2	0.014860	0.014860
0.500	3	0.014860	0.014860
0.600	1	0.014860	0.014860
0.600	2	0.014860	0.014860
0.600	3	0.014860	0.014860
0.700	1	0.014860	0.014860
0.700	2	0.014860	0.014860
0.700	3	0.014860	0.014860
0.800	1	0.014860	0.014860
0.800	2	0.014860	0.014860
0.800	3	0.014860	0.014860
0.900	1	0.014860	0.014860
0.900	2	0.014860	0.014860
0.900	3	0.014860	0.014860
0.950	1	0.014860	0.014860
0.950	2	0.014860	0.014860
0.950	3	0.014860	0.014860

TABLE 1 (CONT)

*** PRESSURE FIELD RESULTS ***

SYMBOLS AND UNITS

EX   AXIAL COORDINATE OF FIELD POINT,
      FRACTION OF RADIUS
ER   RADIAL COORDINATE OF FIELD POINT,
      FRACTION OF RADIUS
TETA ANGULAR COORDINATE OF FIELD POINT,
      RADIANS
NT   NONDIMENSIONAL TIME, NT=TIME*RPM/60
KP   PRESSURE COEFF., P/(DENSITY*((RPM/
      60)**2)*(DIAMETER**2))

EX= -0.8000   ER= 1.2000   TETA= 0.0

1 - TOTAL PRESSURE

NT	KP	
	REAL	IMAG
0.0	0.109260	0.064822
0.0625	-0.002797	0.087227
0.1250	-0.101459	0.032849
0.1875	-0.086291	-0.053374
0.2500	0.115199	-0.156751
0.3125	0.085257	-0.032765
0.3750	0.021487	0.064308
0.4375	-0.051879	0.049902
0.5000	-0.0304070	-0.024493
0.5625	-0.045830	-0.065644
0.6250	0.036785	0.004191
0.6875	0.028781	0.083445
0.7500	-0.047159	0.067708
0.8125	-0.08048	-0.061579
0.8750	0.040268	-0.055254
0.9375	0.117604	0.020541

TABLE 1 (cont)

2 - HARMONIC COMPONENTS

HARM.NO.	KP REAL	IMAG
0	0.000563	0.000171
1	-0.000115	0.001645
2	0.008606	0.000716
3	0.069201	0.047710
4	-0.001695	-0.002692
5	-0.011514	-0.011500
6	-0.010340	0.001098
7	0.000716	0.001721
8	0.010076	0.001721
9	-0.001120	-0.009159
10	-0.000015	0.000259
11	0.000433	0.000063
12	0.019964	-0.009159
13	0.000831	-0.000075
14	-0.000070	-0.000130
15	0.018597	0.007825

TABLE 1 (cont.)

the wake after about 7 revolutions was found negligible, which agrees
with calculation by Kerwin [18] for the zeroth harmonic. For field
points down stream the wake integration is carried down 7 revolutions
beyond the axial position of the field point.

It is shown in Table 2 how the number of chordwise panels and
the angular grid spacing affect the value of the harmonic components
of the pressure.

Figures 9 and 10 show the pressure variation and harmonic
components at the field point due to the zeroth and third harmonic
of loading respectively.

Since we used an arbitrary loading distribution we cannot assess
the accuracy of the results. This will have to be done at a later
date.

	A		B	
No. of panels	15		15	
Grid spacing	4 degrees		2 degrees	

HARM.NO.	K_p REAL	IMAG	K_p REAL	IMAG
0	0.0	0.0	0.0	0.0
3	0.081273	0.054870	0.076421	0.053042
6	-0.014081	0.000345	-0.009018	0.000736
9	0.002288	-0.017413	0.001631	-0.012273

	C
No. of panels	20
Grid spacing	2 degrees

HARM.NO.	K_p REAL	IMAG
0	0.0	0.0
3	0.069201	0.047710
6	-0.010340	0.001098
9	0.001120	-0.009159

TABLE 2 - EFFECT OF NUMBER OF CHORDWISE PANELS

AND ANGULAR GRID SPACING
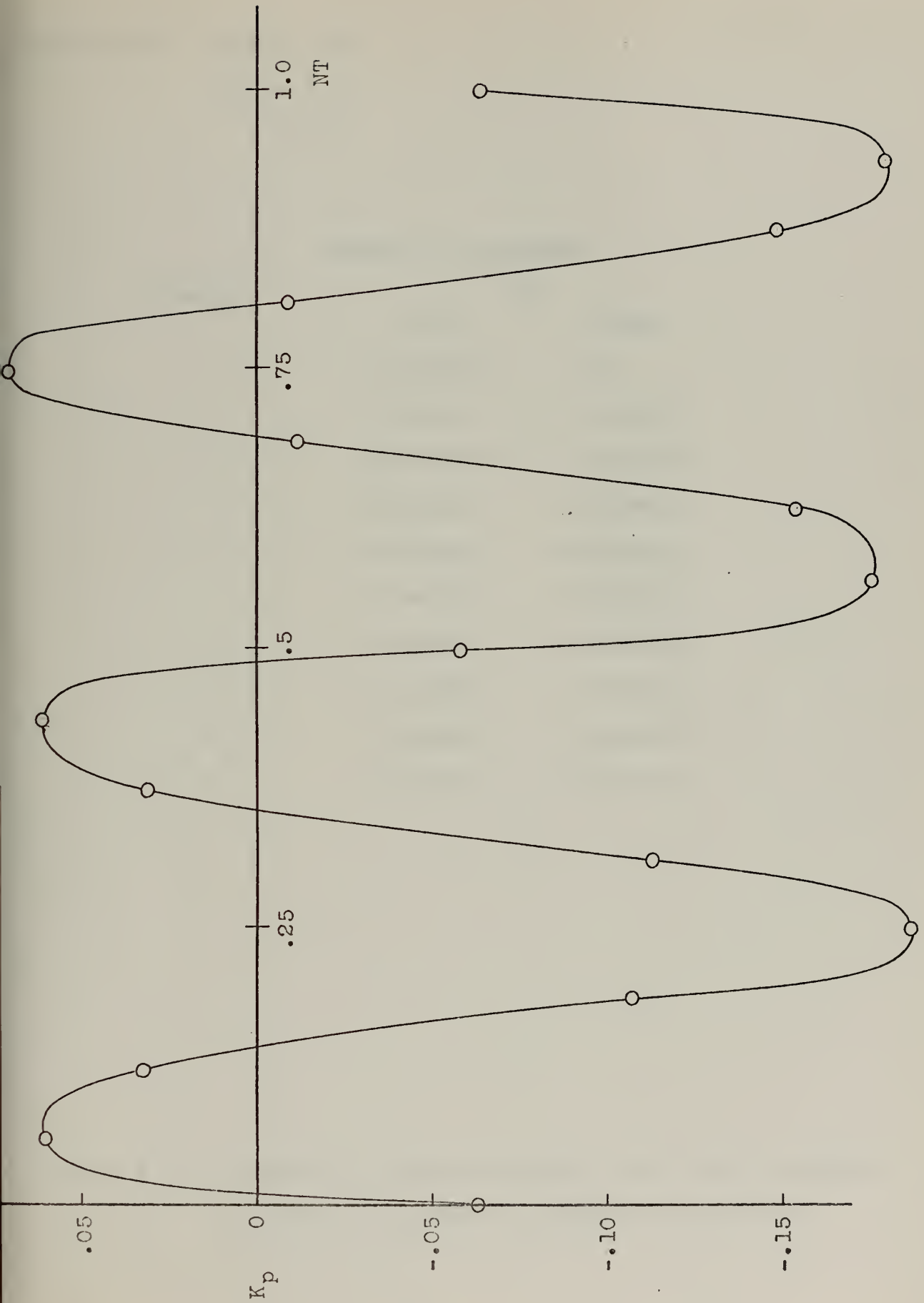
FIG. 9.a - PRESSURE AT UPSTREAM FIELD POINT DUE TO ZEROTH HARMONIC OF LOADING

Field point: x/R = 0.8

r/R = 1.2

0 = 0.

HARMONIC COMPONENTS

HARM.NO.	KP	
	real	imag.
0	-0.059293	0.0
1	-0.000003	-0.000004
2	-0.000002	-0.000002
3	-0.001161	-0.064603
4	-0.000003	-0.000001
5	0.000000	-0.000001
6	-0.000897	-0.000608
7	-0.000006	0.000004
8	0.000000	0.000000
9	-0.000006	-0.000004

FIG. 9.b - PRESSURE AT UPSTREAM FIELD POINT DUE TO ZEROTH

HARMONIC OF LOADING - HARMONIC COMPONENTS

FIG. 10.a - PRESSURE AT UPSTREAM FIELD POINT DUE TO THIRD HARMONIC OF LOADING

O - real part

● - imaginary part

Field point: x/R = 0.8

r/R = 1.2

0 = 0.

.HARMONIC COMPONENTS

HARM.NO.	KP	
	real	imag.
0	0.000563	0.000171
1	-0.000115	0.001645
2	0.008606	0.000716
3	0.069201	0.047710
4	-0.001695	-0.002692
5	-0.001514	-0.001500
6	-0.010340	0.001098
7	0.000716	0.001721
8	0.000076	-0.000898
9	-0.001120	-0.009159

FIG.10.b - PRESSURE AT UPSTREAM FIELD POINT DUE TO

THIRD HARMONIC OF LOADING - HARMONIC

COMPONENTS

Chapter V

CONCLUSIONS AND RECOMMENDATIONS

A computerized procedure has been developed for the calculation of the pressure field generated by a propeller operating in an unsteady flow. We believe that it represents an important improvement over the existing methods based on lifting line theory and circumferentially uniform wake. It is also a useful complement to the recently published work by Jacobs et al. [19] which develops a different approach to the same problem.

A considerable amount of time was put into the optimization of the program but it is probable that it can still be ameliorated. One of the most time consuming operations -- the integration of the streamwise vorticity in the wake -- was successfully reduced by the use of the Euler Transformation. The two other operations whose improvement would have an important effect on the over-all improvement of the program are the integration of the radial vorticity in the wake and the calculation of the velocity potential.

Sample calculations were made to determine the sensibility of the results to the number of chordwise panels, angular grid spacing and how far downstream integrations were carried. Assessment of the accuracy of the results was not possible since we used an arbitrary loading distribution.

Certainly, the next thing that needs to be done is to compare results with experimental data or with the results obtained in [19].

This requires that the loading distribution be obtained by any

of the existing methods referred to before. The program accepts

the input loading distribution in terms of pressure or circulation.

REFERENCES

[1] Kerwin, J.E. and Leopold R., "A Design Theory for Subcavitating Propellers," Trans. SNAME, Vol. 72, 1964.

[2] Brown, N.A., "Periodic Propeller Forces in Non-Uniform Flow," MIT, Dept. NAME, June 1964.

[3] Bjorklund, F.R., "Computation of Periodic Propeller Forces in Non-Uniform Flows Using a Lifting-Surface Model," MIT, Dept. NAME Thesis, 1967.

[4] Cox, B.D. "Workshop on Lifting-Surface Theory in Ship Hydro-dynamics," MIT, Dept. NAME, Report No. 70-8, March 1970.

[5] Landahl, M.T. and Stark, V.J.E., "Numerical Lifting-Surface Theory-Problems and Progress," AIAA Journal, Vol. 6, No. 11, 1968, pp. 2049.

[6] Tsakonas, S. and Jacobs, W.R., "Propeller Loading Distributions," DL Report 1319, Stevens Institute of Technology, August 1968.

[7] Tsakonas, S., Jacobs, W.R. and Rank P., "Unsteady Propeller Lifting Surface Theory with Finite Number of Chordwise Modes," DL Report 1133, Stevens Institute of Technology, December 1966.

[8] Tsakonas, S., Breslin, J.P. and Jen, J., "Pressure Field Around a Marine Propeller Operating in a Wake," DL Report 857, Stevens Institute of Technology, May 1962.

[9] Breslin, J.P. and Tsakonas, S., "Marine Propeller Pressure Field Due to Loading and Thickness Effects," Trans. SNAME, Vol. 67, 1959, pp. 386.

o

[10] Breslin, J.P., "Review and Extension of the Theory for Near-Field Propeller-Induced Vibratory Effects," Fourth Symposium on Naval Hydrodynamics, August 1962.

[11] Breslin, J.P., "The Pressure Field Near a Ship Propeller," J. Ship Research, Vol. 1, No. 4, 1958, pp. 57.

[12] Greenberg, M.D., "The Unsteady Loading on a Marine Propeller in a Non-Uniform Flow," J. Ship Research, Vol. 8, No. 3, 1964, pp. 29.

[13] Laidlaw, W.R., "Theoretical and Experimental Pressure Distributions on Low Aspect Ratio Wings Oscillating in an Incompressible Flow," Aeroelastic and Structures Research Lab, MIT, TR 51-2, 1954.

[14] Ashley, H., Bisplinghoff, R.L. and Halfman, R.L., Aeroelasticity, Addison-Wesley Publishing Co., Massachusetts, 1955.

[15] Verbrugh, P.J., "Unsteady Lifting Surface Theory for Ship Screws," Netherlands Ship Model Basin, Report 68-]36-AH, 1968.

[16] Lamb, H., Hydrodynamics, 6th edition, Dover Publications, N.Y., 1945.

[17] Lewis, F.M., "Propeller Vibration Forces in Single Screw Ships," Trans. SNAME, Vol. 77, 1969.

[18] Kerwin, J.E., "Propeller Blade Section Design," August 1970 (to be published).

[19] Jacobs, W.R., Mercier, J. and Tsakonas, S., "Theory and Measurements of the Propeller-Induced Vibratory Field," DL Report 1485, Stevens Institute of Technology, December 1970.

[20] Squire, N., _Integration for Engineers and Scientists_, American

      Elsevier Publishing Co., New York, 1970.

[21] Abramowitz, M. and Segun, I., _Handbook of Mathematical Functions_,

      Dover Publications, New York, 1965.

[22] Denny, S.B., "Comparisons of Experimentally Determined and

      Theoretically Predicted Pressures in the Vicinity of a Marine

      Propeller," NSRDC Report 2349, May 1967.

[23] _____, "IBM System/360 Scientific Subroutine Package," International

      Business Machines Corp., Data Processing Div., White Plains, N.Y.,

      1968.

Appendix A

VELOCITY POTENTIAL INDUCED BY A SINGLE VORTEX

In this appendix we compare the velocity potential induced by a single reentrant vortex with the one induced by a concentrated doublet of equivalent strength.

The velocity potential due to a vortex is given by

$$\Phi_v = \frac{S}{4\pi} \iint_A \frac{\cos \Psi}{D^2} \, dA \tag{A-1}$$

where

S = vortex strength

A = area enclosed by the vortex

Ψ = angle between the normal to A and the line from A to the field point

D = distance from A to the field point.

Equation (A-1) is similar to the one that gives the velocity potential induced by a uniform distribution over A of source doublets of strength S. It is clear that the strength of the equivalent concentrated doublet must be equal to S $\times$ A.

In order to simplify the calculations, we will consider a rectangular vortex centered at the origin, as shown in Fig. A-1. The velocity potential at p is found using eq. (A-1)

$$\Phi_v = \frac{S}{4\pi} \int_{-a}^{a} \int_{-a}^{a} \frac{z \, d\xi \, d\eta}{[(x-\xi)^2 + (y-\eta)^2 + z^2]^{\frac{3}{2}}}$$
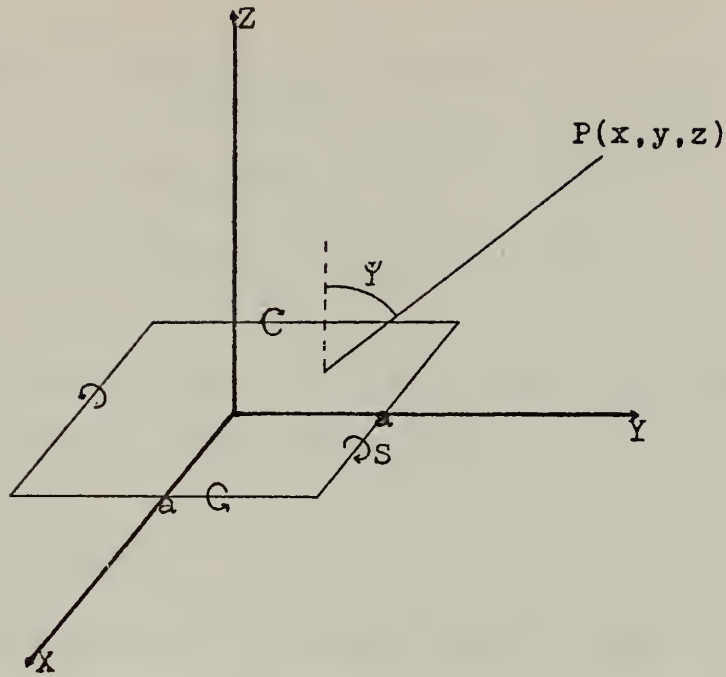
FIG. A-1 - ORIENTATION OF REENTRANT VORTEX

The above integral can be evaluated analytically by integrating directly in one of the variables -- ξ, say -- and then making the following changes of variables before performing the next integration:

$$v = \frac{\eta - y}{[(x \quad a)^2 + z^2]^{\frac{1}{2}}}$$

$$u = v + (v^2 + 1)^{\frac{1}{2}}$$

$$t = u^2$$

The final result is

$$\Phi_v = \frac{S}{4\pi} \left[(\tan^1 A - \tan^1 B) - (\tan^1 C - \tan^1 D) \right] \tag{A-2}$$

where

$$A = \frac{(y+a)^2 + z^2 - (y-a)[(x+a)^2 + (y-a)^2 + z^2]^{\frac{1}{2}}}{z(x+a)}$$

$$B = \frac{(y+a)^2 + z^2 - (y+a)[(x+a)^2 + (y+a)^2 + z^2]^{\frac{1}{2}}}{z(x+a)}$$

$$C = \frac{(y-a)^2 + z^2 - (y-a)[(x-a)^2 + (y-a)^2 + z^2]^{\frac{1}{2}}}{z(x-a)}$$

$$D = \frac{(y+a)^2 + z^2 - (y+a)[(x-a)^2 + (y+a)^2 + z^2]^{\frac{1}{2}}}{z(x-a)}$$

The velocity potential induced at p by a concentrated doublet of strength $4a^2S$, located at the origin is given by

$$\Phi_d = \frac{a^2 S z}{\pi(x^2 + y^2 + z^2)^{\frac{3}{2}}} \tag{A-3}$$

It is physically reasonable to predict that the largest differences between the values given by eqs. (A-1) and (A-2) will be found at the field points lying on the z axis. Figure A-2 shows how those differences vary with the distance along the z axis.

It is apparent from the analysis of Fig. A-2 that the ratio of the two values approaches very rapidly the unity. For z/a = 8 (i.e., for a distance 4 times greater than the side of the original vortex) the difference between the two values is less than one percent.
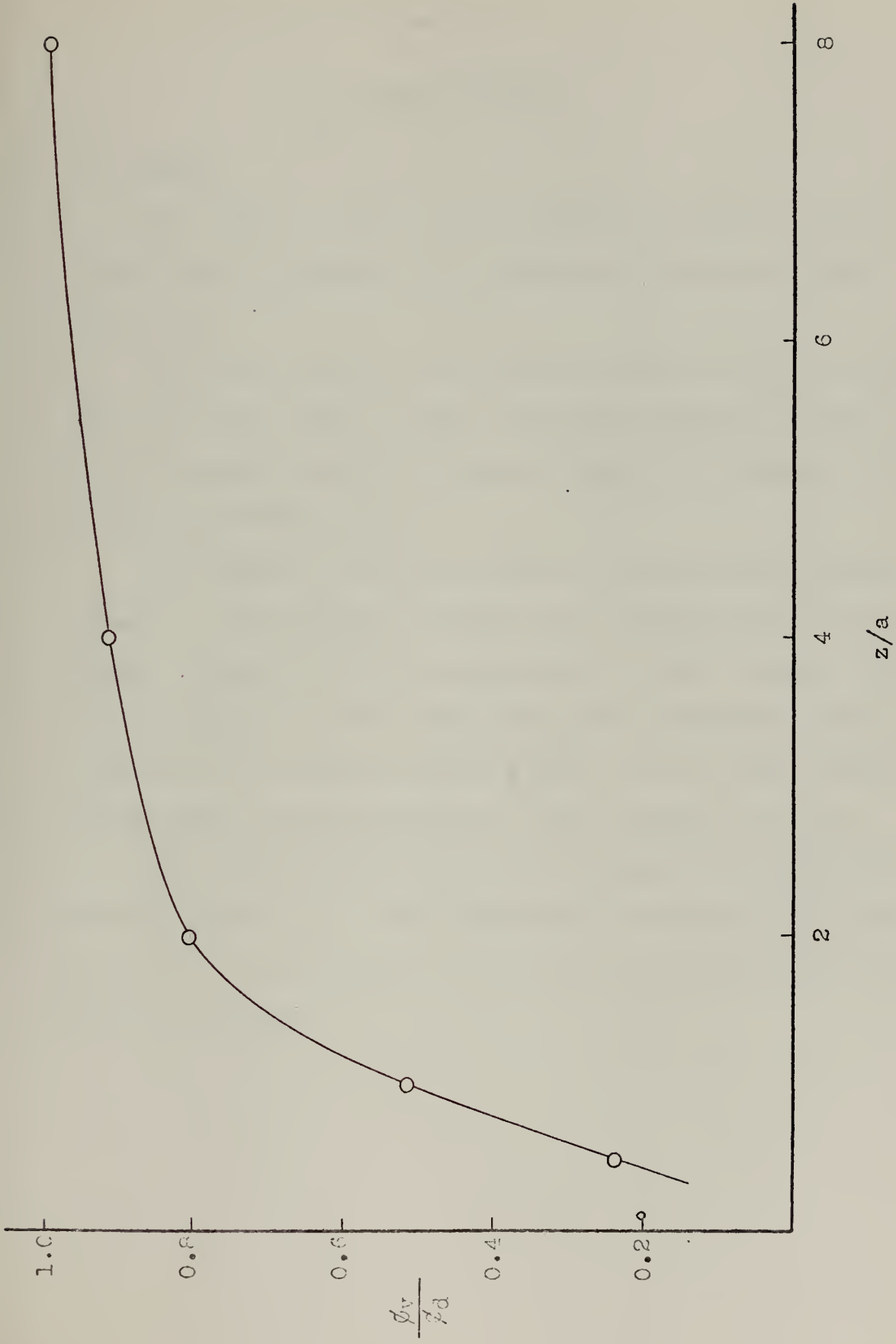
FIG. A-2 - COMPARISON OF THE VELOCITY POTENTIAL INDUCED BY A REENTRANT VORTEX AND
BY A DOUBLET OF EQUIVALENT STRENGTH

Appendix B

COMPUTER PROGRAM

1. <u>General</u>

The program presented in this appendix is essentially the
translation into FORTRAN IV of the numerical solution outlined in
Chapter III.

The initial section of the program in which the blade and wake
are divided into panels is taken from Professor Kerwin's program, [18].
Also, the scheme used for the zeroth harmonic of the loading is based
on Professor Kerwin's work.

The program is written for use on the IBM System/360 digital
computer. For different processors slight changes might have to be
made. The amount of memory space required is about 150K bytes and
the computation time for a single field point, including harmonic
analysis of the pressure is about 2 minutes for the zeroth harmonic
and 5 minutes for higher harmonics, using a FORTRAN G Compiler.

The complex harmonic analysis is performed by the subroutine
HARM described in [23]. The final output variables are subscripted.
This was done in anticipation of a plotting subroutine which can be
added in the future.

2. List of Key Variables

The following is a list of the principal variables in the program, arranged in alphabetical order.

A(M,N)   = Coefficients of the Birnbaum modes of the loading function

BOUNDA   = Axial velocity of the field point, induced by the bound vortices

BOUNDT   = Tangential velocity at the field point, induced by the bound vortices

BWAKEA   = Axial velocity at the field point, induced by the radial vortices in the wake

BWAKET   = Tangentical velocity at the field point, induced by the radial vortices in the wake

CHOR(M) = Local chord at radius R(M)

DHUB   = Hub diameter

DIAM   = Propeller diameter

ER   = Radial position of the field point

EX   = Axial position of the field point

G(M)   = Chordwise integral of the bound circulation at radius R(M)

GB(M,N) = Bound circulation assumed concentrated on the N'th grid line in the M'th chordwise panel

GL(M,N) = Wake circulation assumed concentrated between the KWAKE(M) + N and KWAKE(M) + N + 1 grid lines in the M'th chordwise panel, for computing PTWK

GLR(M)   = Advance coefficient at radius R(M)

GLS   =   Advance coefficient based on VS

GP   =   Circulation in the blade, assumed concentrated in the

              middle of each element of the lattice for computing PTBL

GR   =   Radial circulation in the wake

GT(M,N)   =   Streamwise circulation in the blade, between the N and

              N + 1 grid lines in the M'th panel

IDENT   =   Identification of the propeller

IGB   =   Parameter that describes the loading function. If IGB = 0

              the loading is in terms of bound circulation; if IGB > 0

              it is in terms of the pressure jump in the blade

KD(N)   =   Angle between the N'th blade and the YY axis

KN(M)   =   Reduced frequency at radius R(M)

KWAKE(M) =   Identification of the first grid line of the wake ar

              radius RZ(M)

MN   =   Number of equal spaces in the division of the span into

              chordwise panels

NBLADE   =   Number of blades

NHARM   =   Harmonic number

NL   =   Largest integer multiple of the grid spacing with value

              less or equal to TMIN

NLE(M)   =   Identification of the first grid line in the M'th panel

NMAX   =   Number of loading modes

NR   =   Largest integer multiple of the grid spacing with value

              less or equal to TMAX

NT   =   Total number of grid lines in the blade

NTE(M)   =   Identification of the last grid in the blade in the M'th panel

NTH   =   Parameter that defines the spacing between grid lines as
                  NTH X 2 degrees

NVV(M)   =   Total number of grid lines spanned by the blade in the
                  M'th panel

PHN(M)   =   Phase angle of the NHARM'th harmonic of the inflow velocity

PRS(M)   =   Field point pressure when the first blade is at an angle
                  of $M*\pi/(8\ NBLADE)$ with fixed vertical axis

PTBL   =   Time derivative of the velocity potential at the field
                  point, induced by the circulation in the blade

PTWK   =   Time derivative of the velocity potential at the field
                  point, induced by the circulation in the wake

PTSC   =   Time derivative of the velocity potential at the field
                  point, induced by the source distribution

R(M)   =   Midradius of the M'th chordwise panel

RPM   =   Rotation per minute

RZ(M)   =   Radius at the lower bound of the M'th panel

SB(M,N)   =   Source strength concentrated on the N'th grid line in
                  the M'th chordwise panel

SL(M)   =   Leading edge at radius R(M)

SMA(N)   =   Differential of the thickness at the N'th grid line, as
                  percent of the max thickness in each panel

SOURCA   =   Axial velocity at the field point, induced by the source
                  distribution

SOURCT   =   Tangential velocity at the field point, induced by the
                  source distribution

ST(M)   = Trailing edge at radius R(M)

STAR(M)   = Factor which multiplied by SMA(N) gives the source strength
                 at the N'th grid line in the M'th chordwise panel

TETA   = Angular coordinate of the field point

TK(N)   = Standard thickness, fraction of the max thickness

TL(M)   = Amplitude of the streamwise vorticity in the wake at
                 radius RZ(M)

TLE(M)   = Angular coordinate of the leading edge at radius R(M)

TMAX   = Extreme value of TTE(M) over all the panels

TMIN   = Extreme value of TLE(M) over all the panels

TRAILA   = Axial velocity at the field point, induced by the
                 streamwise vorticity in the blade

TRAILT   = Tangential velocity at the field point, induced by the
                 streamwise vorticity in the blade

TTE(M)   = Angular coordinate of the trailing edge at radius R(M)

TWAKEA   = Axial velocity at the field point, induced by the stream-
                 wise vorticity in the wake

TWAKET   = Tangential velocity at the field point, induced by the
                 streamwise vorticity in the wake

VFP   = Inflow velocity at the field point

VS   = Ship speed

VXO(M)   = Zeroth harmonic of the inflow velocity at radius R(M)

XGL(N)   = Advance coefficient at radius XR(N)

XKN(N)   = Reduced frequency at radius XR(N)

XPHN(N)   = Phase angle of the NHARM'th harmonic of the inflow

        velocity at radius XR(N)

XR(N)   = Input radius (see Input Description)

XSL(N)   = Leading edge at radius XR(N)

XST(N)   = Trailing edge at radius XR(N)

XSTAR(N) = Factor of proportionality of the source strength at

        radius XR(N)

XTBETA(N) = Tangent of the advance angle at radius XR(N)

XTZ(N)   = Maximum thickness at radius XR(N)

XVXN(N) = NHARM'th harmonic of the inflow velocity at radius XR(N)

3. Input Description

The following sequence of input cards is required for the operation of the program:

A	IDENTIFICATION	1 card
B	GENERAL DESCRIPTION	1 card
C	BLADE OUTLINE	3 cards
D	WAKE CHARACTERISTICS	4 cards
E	LOADING DISTRIBUTION	21 cards max.
F	FIELD POINT DESCRIPTION	1 card

A complete description of the above input cards is presented in Table B-1. The input radii referred to in that table are schematically shown in the figure below.
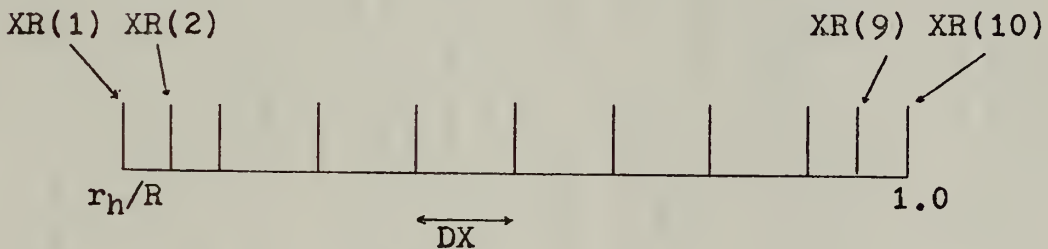
FIG. B-1 - INPUT RADII OF PROPELLER DATA

DX is the Input Spacing, equal to $\frac{1}{8}$ X interval from hub to tip.

Table B1

INPUT FORM

Card No Type Req'd	Description of Contents	Var. Name	Format	Card Col.
A 1	Propeller identification	IDENT	18A4	1-72
B 1	RPM	RPM	F8.4	1-8
	Ship speed, knots	VS	F8.4	9-16
	Diameter, inches	DIAM	F8.4	17-24
	Hub diameter, inches	DHUB	F8.4	25-32
	No of blades	NBLADE	I3	33-35
	No. of equal divisions of the span	MN	I3	36-38
	Grid Spacing	NTH	I3	39-41
C	Table of offsets (given at input radii XR(1) to XR(10) - see text)			
1	Leading edge, inches (negative if upstream of reference line)	XSL	10F7.5	1-70
1	Trailing edge, inches (positive if downstream of reference line)	XTL	10F7.5	1-70
1	Thickness, inches (for linear taper give values at hub and tip on two first spaces and leave the rest blank)	XTZ	10F7.5	1-70
D	Inflow components at radii XR(1) to XR(9)			
1	Velocity of zeroth harmonic, fraction of ship speed	XVXO	9F8.4	1-72
1	Harmonic number	NHARM	I3	1-3
1	Amplitude of harmonic component correspondent to NHARM, fraction of ship speed	XVXN	9F8.4	1-72
1	Phase of harmonic component correspondent to NHARM, radians	XPHN	9F8.4	1-72
E 1	Type of loading (if eq. zero - given by vortex distribution, if g.t. zero - given by pressure distribution)	IGB	I3	1-3
	Number of loading modes (max is 10)	NMAX	I3	4-6
2 per mode	Complex loading coefficients at radii XR(1) to XR(9). Units: $ft^2 \times sec^{-1}$ if IGB = 0, $lb \times ft^{-2} \times slug^{-1}$ if IGB > 0	A	9F8.4	1-72
F 1	x coord. of field point, fraction of radius	EX	F8.4	1-8
	r coord. of field point, fraction of radius	ER	F8.4	9-16
	θ coord. of field point, fraction of radius	TETA	F8.4	17-24
	Free stream velocity at field point, fraction of ship speed	VFP	F8.4	25-32

4. Program Listings

```fortran
C *** ************* MAIN PROGRAM ***********************************
C
      REAL KN,KD
      COMPLEX A,CF,SB,GB,G,TRL,GT,TL,EXK,BOUNDA,
     1 BOUNDT,SOURCA,SOURCT,TRAILA,TRAILT,SP,RAT,BWAKEA,
     2 BWAKET,TWAKFA,TWAKET,CAT,GR,GL,PTBL,GP,PTWK,PTSC,
     3 PRS,FWA,FWT,FITTIN,AKA,AKT,BKA,BKT,CKA,CKT,DKA,
     4 DKT,EKA,FKT,ASUMA,ASUMT,BVORT,CEXP,ZTEMP
      DIMENSION XGL(9),XSTAR(9),XKN(9),R(25),RZ(25),ST(25),
     1 SL(25),GLR(25),STAR(25),ROOT(25),TLE(25),TTE(25),
     2 SB(25,75),GB(25,75),NLE(25),NTE(25),NVV(25),
     3 CHOR(25),G(25),X(75),SMA(75),KWAKE(25),RZSQ(25),
     4 GT(25,75),TL(25),KD(10),EXK(10),GL(25,250),
     5 PRS(16),AKA(10),AKT(10),BKA(4),BKT(4),CKA(3),
     6 CKT(3),DKA(2),DKT(2),INV(4),SS(4),NI(16),PHN(25)
      COMMON/Q1/IDENT(18),XR(10),XSL(10),XST(10),XTZ(10),
     1 XTRETA(9),XVXO(9),XVXN(9),XPHN(9),DIAM,DHUB,RPM,
     2 DELT,NBLADE,NHARM,MT/Q2/A(25,10),VXO(25),KN(25),VS,IGB,
     3 NMAX/Q3/NDK(199),IDK(66),Z(17),TK(17),XMP(10),NV(3)/Q4/KK,
     4 DK,XU,FX,ER,TETA,ALFA,GLCV,AR
      EXTERNAL FWA,FWT
C
C THIS SECTION OF THE MAIN PROGRAM READS THE INPUT, NON-
C DIMENSIONALIZES IT AND ADAPTS IT TO THE LATTICE
C
    9 READ(5,3) IDENT,RPM,VS,DIAM,DHUB,NBLADE,MN,NTH,
     1 XSL,XST,XTZ,XVXO,NHARM,XVXN,XPHN,IGB,NMAX,
     2 ((A(I,J),I=1,9),J=1,NMAX)
    3 FORMAT(18A4/4F8.4,3I3/10F7.5/10F7.5/10F7.5/9F8.4/
     1 I3/9F8.4/9F8.4/2I3/(9F8.4))
      STEMP=NHARM
      CF=(0..0.1f462)*STEMP*RPM
      ROVER=2.0/DIAM
      RH=DHUB/DIAM
      DX=1..125*(1.0-RH)
      XR(1)=RH+0.5*DX
```

```
   XR(5)=1.0-0.5*DX
   XR(2)=RH+DX
   XR(1)=1.0
   DO 2 N=3,8
 2 XR(N)=XR(N-1)+DX
   DO 5 N=1,17
   XSL(N)=XSL(N)*ROVER
 5 XST(N)=XST(N)*ROVER
   GLS=387.67*VS/RPM/DIAM
 6 DELT=0.3495.66*FLOAT(NTH)
   DOF=0.25*DELT
   IF(XTZ(3).GT.0.0) GO TO 11
   BUG=(XTZ(1)-XTZ(2))/(1.0-RH)
   MOUSE=XTZ(1)
   DO 15 N=1,9
15 XTZ(N)=MOUSE-BUG*(XR(N)-RH)
11 BUG=ROVER/VS/0.8843075
   DO 10 N=1,9
   XTZ(N)=XTZ(N)*ROVER
   XTBETA(N)=GLS*XVX2(N)/XR(N)
   XGL(N)=XR(N)*XTBETA(N)
   XSTAR(N)=XTZ(N)*XVXN(N)*SQRT(XR(N)**2+
  1 XGL(N)**2)/XGL(N)/6.28318
   XKN(N)=0.0025836*STEMP*RPM*(XST(N)-XSL(N))/
  1 (ROVER*VS*XVXD(N))
10 A(N,I)=A(N,I)*BUG
   DO 10 I=1,NMAX
   MT=MN+4
   CALL OUTPUT
   MAX=MT+1
   DELM=(1.0-RH)/MN
   BUG=0.625*DELM
   RZ(1)=RH+BUG
   RZ(MAX)=1.0-BUG
   BUG=0.25*DELM
   RZ(2)=RH+BUG
```

```
      R7(MT)=1.0-BUG
      BUG=0.5*DELM
      RZ(3)=RH+BUG
      R7(MN+3)=1.0-BUG
      R7(MN+2)=1.0-DELM
      BUG=.125*DELM
      R(1)=RH+BUG
      R(MT)=1.0-BUG
      BUG=.375*DELM
      R(2)=RH+BUG
      R(MN+3)=1.0-BUG
      BUG=.75*DELM
      R(3)=RH+BUG
      R(MN+2)=1.0-BUG
      DO 12 M=3,MN
      R(M+1)=(M-1.5)*DELM+RH
   12 R7(M+1)=(M-2)*DELM+RH
      DO 2 M=1,MT
      RMAP=ARCOS((1.0+RH-2.0*R(M))/(1.0-RH))
      ST(M)=FILLIN(RMAP,XMP,XST,10)
      SL(M)=FILLIN(RMAP,XMP,XSL,10)
      GLR(M)=FILLIN(R(M),XR,XGL,9)
      VX(M)=FILLIN(R(M),XR,XVX5,9)
      KN(M)=FILLIN(R(M),XR,XKN,9)
    o PHN(M)=FILLIN(R(M),XR,XPHN,9)
      STAR(M)=FILLIN(R(M),XR,XSTAR,9)
      DO 22 N=1,NMAX
      A(M,N)=FITTIN(R(M),XR,A,N,9)
   2? CONTINUE
      GIR(MAX)=GLR(MT)
      TMIN=0.0
      TMAX=2.0
      DO 23 M=1,MT
      ROOT(M)=SQRT(R(M)**2+GLR(M)**2)
      TLF(M)=SL(M)/ROOT(M)
      TTE(M)=ST(M)/ROOT(M)
```

```
      TMIN=AMIN1(TMIN,TLE(M))
23    TMAX=AMAX1(TMAX,TTE(M))
      ROOT(MAX)=ROOT(MT)
      NL=-TMIN/DELT
      NR=TMAX/DELT
      NT=NL+NR+1
      IF(NT.LT.74) GO TO 7
      NTH=NTH+1
      GO TO 6
7     DO 21 N=1,NT
      DO 21 M=1,MAX
      SR(M,N)=(0.0.0.)
21    GR(M,N)=(0.0.0.)
      DO 26 M=1,MT
      NLF(M)=INT(TLE(M)/DELT)+NL+1
      NTE(M)=INT(TTE(M)/DELT)+NL+1
      NVV(M)=NTE(M)-NLE(M)+1
      XL=(-TLE(M)+(NLE(M)-NL-1)*DELT)*ROOT(M)
      CHOR(M)=ST(M)-SL(M)
      IF(NVV(M)-1) 99,25,42
42    D=DELT*ROOT(M)
      G(M)=(0.0.0.)
      X(1)=0.
      X(2)=XL+0.5*D
0     IF(NVV(M).LT.3) GO TO 52
      NVM=NVV(M)
.     DO 51 N=3,NVM
51    X(N)=X(N-1)+D
52    X(NVV(M)+1)=CHOR(M)
      NMIN=NVV(M)-1
      BUG=0.
      DO 34 N=1,NMIN
      PP=FILLIN(X(N+1)/CHOR(M),Z,TK,17)
      SMA(N)=PP-BUG
34    BUG=PP
      SMA(NVV(M))=-BUG
```

```
      DO 24 N=1,NVM
      SR(M,N)=STAR(M)*SMA(N)*CEXP((0.,1.)*PHN(M))
      BUG=ARCOS(1.0-2.0*(XL+(N-1)*D)/CHOR(M))
      IF(XL.EQ.0.0) GO TO 24
343   GR(M,N)=BVORT(M,BUG)*(X(N+1)-X(N))
24    G(M)=G(M)+GB(M,N)
      GO TO 26
75    BUG=ARCOS(1.0-2.0*XL/CHOR(M))
      GR(M,1)=BVORT(M,BUG)*CHOR(M)
      SR(M,1)=STAR(M)*SMA(1)
      G(M)=G(M)+GB(M,1)
26    CONTINUE
      NLE(MAX)=0.
      NTE(MAX)=0.
      KWAKE(1)=NTE(1)
      DO 81 M=2,MAX
81    KWAKE(M)=MAX0(NTE(M-1),NTE(M))
      DO 31 M=1,MAX
      R7SQ(M)=R7(M)**2
      TRL=(0.,0.)
      IMAX=KWAKE(M)-NLE(M)+1
      DO 33 N=1,IMAX
      GT(M,N)=TRL
      IF(M.EQ.MAX) GO TO 32
      GT(M,N)=GT(M,N)-GB(M,N)
      IF(M.EQ.1) GO TO 33
32    GT(M,N)=GT(M,N)+GB(M-1,N)
33    TRL=GT(M,N)
      TL(M)=GT(M,IMAX)
31    CONTINUE
      KD(1)=0.0
      FXK(1)=(1.,0.)
      DO 35 K=2,NBLADE
      KD(K)=6.283185*(K-1)/NBLADE
      RTEMP=STEMP*KD(K)
7     TEMP=RTEMP
```

```
   35 EXK(K)=CEXP((0..-1.)*ZTEMP)
   41 READ(5,49) EX,ER,TETA,VFP
   49 FORMAT(4F8.4)
      WRITE(6,9.) EX,ER,TETA
   9  FORMAT(////19X,'EX=',F8.4,3X,'ER=',F8.4,3X,'TETA=',F8.4)
      WRITE(6,9(0))
   9  FORMAT(//24X,'1 - TOTAL PRESSURE'//
     1 21X,'INT',15X,'RP'/
     2 31X,'REAL',8X,'IMAG'/)
C
C  THIS SECTION OF THE MAIN PROGRAM FINDS THE PERTURBA-
C  TION VELOCITIES AT THE FIELD POINT DUE TO THE
C  SOURCE AND VORTEX DISTRIBUTIONS
C
      DTETA=3.14159/(4.*NBLADE)
      ITETA=0
      TETA=TETA-DTETA
   53 TETA=TETA+DTETA
      ITETA=ITETA+1
      BOUNDA=(0.,0.)
      BOUNDT=(0.,0.)
      SOURCA=(0.,0.)
      SOURCT=(0.,0.)
      TRAILA=(0.,0.)
      TRAILT=(0.,0.)
      DO 38 M=1,MAX
      GLCV=GLR(M)
      IMAX=KWAKF(M)-NLE(M)+1
      DO 38 I=1,IMAX
      PHI=(I+NLE(M)-NL-2)*DELT
      AA=EX-GLCV*PHI
      AB=AA**2+ER**2
      DO 38 K=1,NBLADE
      ANGL=PHI+KD(K)-TETA
      COSIKN=COS(ANGL)
      SINIKN=SIN(ANGL)
```

```
      BB=-2.* ER*COSIKN
      AC=4.*3*(AA**2+(ER*SINIKN)**2)
      IF(N.EQ.MAX) GO TO 71
      IF(I.GT.(NTE(M)-NLE(M)+1)) GO TO 71
      AG=?.0
      AH=?.0
      AI=0.0
      MD=M+1
      BUG=-1.0
      DO 43 N=M,MD
      AE=AC*SQRT(RZSQ(N)+RZ(N)*BB+AB)
      AD=(2.*.*RZ(N)+BB)/AE
      AF=-(BB*RZ(N)+2.0*AB)/AE
      AG=AG+BUG*AD
      AH=AH+BUG*AD
      AI=AI+BUG*AF
   43 BUG=-BUG
      RTEMP=PHI+KD(K)
      RTEMP=STEMP*RTEMP
    7 TEMP=RTEMP
      SP=(1.,-1.)*7TEMP
      BOUNDA=BOUNDA-ER*SINIKN*AG*GB(M,I)*EXK(K)
      BOUNDT=BOUNDT-AA*COSIKN*AG*GB(M,I)*EXK(K)
      SOURCA=SOURCA+AA*AH*SB(M,I)*CEXP(SP)
      SOURCT=SOURCT-SINIKN*AI*SB(M,I)*CEXP(SP)
   71 IF(I.EQ.1) GO TO 22
      IF(I.EQ.IMAX) GO TO 44
      RAT=GT(M,I-1)+GT(M,I)
      GO TO 45
   22 RAT=GT(M,I)
      GO TO 45
   44 RAT=GT(M,I-1)
   45 IF(CABS(RAT).EQ.0.0) GO TO 38
      RTEMP=SQRT((AB+BB*RZ(M)+RZSQ(M))**3)
    7 TEMP=RTEMP
      RAT=RAT*EXK(K)/ZTEMP
```

```
      TRAILA=TRAILA+RZ(M)*(RZ(M)-ER*COSIKN)*RAT
      TRAILT=TRAILT+(-RZ(M)*(GLCV*COSIKN-AA*SINIKN)+
    1 FR GLCV)*RAT
 38 CONTINUE
      TRAILA=TRAILA*DOF
      TRAILT=TRAILT*DOF
      BWAKFA=( . .  . )
      BWAKET=(  . . 0 . )
      TWAKEA=( 0 . 0 . )
      TWAKET=( . . 0 . )
      XL =
      IF(NHARM.NE. ) XU=3.14159/STEMP
      DO 72 M=1.MAX
      GLCV=GLR(M)
      D=DELT*ROOT(M)
      IF(NHARM.NE. ) GO TO 70
      DO 54 K=1.NBLADE
      J=
 73 J=J+1
      IF(J.GT.7( ) GO TO 99
      PHI=(J+KWAKE(M)-NL-2)*DELT
      ANGL=PHI+KD(K)-TETA
      COSIKN=COS(ANGL)
      SINIKN=SIN(ANGL)
      RB=-2. *ER*COSIKN
      AA=EX-GLCV*PHI
      AR=AA**2+ER**2
      BUG=SQRT((AB+RB*RZ(M)+RZSQ(M))**3)
      IF(J.NE. 1) GO TO 5
      RAT=TL(M)/BUG
      GO TO 29
 5  RAT=TL(M)*2. /BUG
 29 TWAKEA=TWAKEA+RZ(M)*(RZ(M)-ER*COSIKN)*RAT*EXK(K)
      TWAKET=TWAKET+(-RZ(M)*(GLCV*COSIKN-AA*SINIKN)+
    1 FR*GLCV)*RAT*EXK(K)
      IF(EX.GT.(XGL(5)*PHI)) GO TO 73
```

```fortran
      DO 54 IWK=1,65
      JJ=J+IDK(IWK)
      PHI=(JJ+KWAKE(M)-NL-2)*DELT
      ANGL=PHI+KD(K)-TETA
      COSIKN=COS(ANGL)
      SINIKN=SIN(ANGL)
      BB=-2.*FR*COSIKN
      AA=EX-GLCV*PHI
      AB=AA**2+ER1**2
      BUG=SQRT((AB+BB*RZ(M)+RZSQ(M))**3)
      RAT=TL(M)*(IDK(IWK)+IDK(IWK+1))/BUG
      TWAKEA=TWAKEA+RZ(M)*(RZ(M)-ER*COSIKN)*RAT*EXK(K)
      TWAKET=TWAKET+(-RZ(M))*(GLCV*COSIKN-AA*SINIKN)+
   54 1 FR*GLCV)*RAT*EXK(K)
      GO TO 72
   7? IF(M.EQ.MAX) GO TO 631
      XT=-ST(M)+(KWAKE(M)-NL-1)*D
      IF(M.NE.1) GO TO 8?
      MM=INT(MAX/2.)
      J=?
   27 J=J+1
      IF(J.GT.7??) GO TO 99
      PHI=(J+KWAKE(MM)-NL-2)*DELT
      IF(EX.GT.(XGL(5)*PHI)) GO TO 27
      JRFF=J
      IWKMAX=JREF+65
      IAKMAX=INT(JREF*DELT/3.14159*NHARM+8.8*NHARM)
   8? I=KWAKE(M)
      RTEMP=STEMP/ROOT(M)
    7 TEMP=RTEMP
      CAT=(i.-i.)*ZTEMP
      DO 63 IWK=1.IWKMAX
      IF(IWK.GT.JREF) GO TO 55
      I=i+IWK
      GO TO 57
   55 I=I+IDK(IWK-JREF)
```

```
57  PHI=(I-NL-2)*DELT
    AA=EX-GLCV*PHI
    AR=AA**2+ER**2
    DO 63 K=1,NBLADE
    ANGL=PHI+KD(K)-TETA
    COSIKN=COS(ANGL)
    SINIKN=SIN(ANGL)
    BB=-2.*ER*COSIKN
    AC=4.*(AA**2+(ER*SINIKN)**2)
    RTEMP=I-KWAKE(M)-1
    RTEMP=(XT/ROOT(M)+RTEMP*DELT)*STEMP
7   TEMP=RTEMP
    SP=(...-1.)*ZTEMP
    BUG=SQRT((AR+BB*RZ(M)+RZSQ(M))**3)
    IF(IWK.NE.1) GO TO 28
    GR=G(M)*CEXP(SP)*(XT+0.5*D)*CAT
    GL(M,IWK)=GR+G(M)
    GO TO 58
28  IF(IWK.GT.JREF) GO TO 59
    GR=G(M)*CEXP(SP)*D*CAT
    GO TO 62
59  RTEMP=IDK(IWK-JREF)+IDK(IWK-JREF+1)
    RTEMP=0.5*D*RTEMP
    ZTEMP=RTEMP
    GR=G(M)*CEXP(SP)*ZTEMP*CAT
62  GI(M,IWK)=GR+GL(M,IWK-1)
58  AG=0.
    AH=0.
    AI=0.
    MD=M+1
    BUG=-1.
    DO 39 N=M,MD
    AE=AC*SQRT(AB+BB*RZ(N)+RZSQ(N))
    AD=(2.*RZ(N)+BB)/AE
    AF=-(BB*RZ(N)+2.0*AB)/AE
    AG=AG+BUG*AD
```

```
      AH=AH+RUG*AD
      AI=AI+RUG*AF
30    RUG=-BUG
      BWAKEA=BWAKEA-AA*COSIKN*AG*GR*EXK(K)
      BWAKET=BWAKET-ER*SINIKN*AG*GR*EXK(K)
63    CONTINUE
631   DO 76 K=1,NBLADE
      IF(CABS(TL(M)).EQ.0.0) GO TO 76
      DO 75 IWK=1,IAKMAX
      KK=IWK-1
      ALFA=(KWAKE(M)-N1-1)*DELT
      DK=KD(K)
      AP=RZ(M)
      CALL QG5(XL,XU,FWA,AKA(IWK))
75    CALL QG5(XL,XU,FWT,AKT(IWK))
      DO 64 J=1,4
      BKA(J)=-AKA(IAKMAX-5+J)+AKA(IAKMAX-4+J)
64    BKT(J)=-AKT(IAKMAX-5+J)+AKT(IAKMAX-4+J)
      DO 66 J=1,3
      CKA(J)=-BKA(J)+BKA(J+1)
66    CKT(J)=-BKT(J)+BKT(J+1)
      DO 67 J=1,2
      DKA(J)=-CKA(J)+CKA(J+1)
67    DKT(J)=-CKT(J)+CKT(J+1)
      EKA=-DKA(1)+DKA(2)
      EKT=-DKT(1)+DKT(2)
      ASUMA=(0.,0.)
      ASUMT=(0.,0.)
      JMAX=IAKMAX-5
      DO 74 J=1,JMAX
      ASUMA=ASUMA+AKA(J)
74    ASUMT=ASUMT+AKT(J)
      RAT=ASUMA/2.-BKA(1)/4.+CKA(1)/8.-DKA(1)/16.+EKA/32.
      CAT=ASUMT/2.-BKT(1)/4.+CKT(1)/8.-DKT(1)/16.+EKT/32.
      SP=(0.,1.)*(ALFA-DK)
      TWAKEA=TWAKEA+TL(M)*CEXP(SP)*RAT/2.
```

```
        TWAKET=TWAKET+TL(M)*CEXP(SP)*CAT/2.
76  CONTINUE
77  CONTINUE
        IF(NHAFM.NE.0) GO TO 720
        TWAKFA=TWAKEA*DOF
        TWAKET=TWAKET*DOF

C  THIS SECTION OF THE MAIN PROGRAM FINDS THE TIME DERI-
C  VATIVE OF THE VELOCITY POTENTIAL AT THE FIELD POINT
C  DUE TO THE SOURCE AND VORTEX DISTRIBUTIONS
C

720  PTBL=(0.,0.)
        PTWK=(0.,0.)
        PTSC=(0.,0.)
        IF(NHARM.EQ.0) GO TO 96
        DO 68  M=1.MT
        GLCV=GLR(M)
        RAT=(0.,0.)
        GP=(0.,0.)
        VTEMP=ROOT(M)*(RZ(M+1)-RZ(M))
        NVM=NVV(M)
        DO 65  I=1.NVM
        PHI=(I+NLE(M)-NL-1.5)*DELT
        AA=EX-GLCV*PHI
        AB=AA**2+ER**2
        DO 65  K=1.NBLADE
        ANGL=PHI+KC(K)-TETA
        COSIKN=COS(ANGL)
        BB=-2.*ER*COSIKN
        RUG=(AA*R(M)+ER*COSIKN*GLCV)/ROOT(M)
        GP=GP+GR(M.I)*EXK(K)
        RTEMP=RUG/SQRT((AB+R(M)*(R(M)+BB))**3)
        RTEMP=RTEMP
65  RAT=RAT+GP*ZTEMP
        ZTEMP=VTEMP
        PTBL=PTBL+RAT*ZTEMP
```

```
      I=KWAKE(M)
      RAT=(1.,0.)
      DO 651 IWK=1,IWKMAX
      IF(IWK.GT.JREF) GO TO 652
      I=I+IWK
      GO TO 653
  652 I=I+IDK(IWK-JREF)
  653 PHI=(I-NL-1.5)*DELT
      AA=EX-GLCV*PHI
      AB=AA**2+ER**2
      DO 651 K=1,NBLADE
      ANGL=-PHI+KD(K)-TETA
      COSIKN=COS(ANGL)
      BB=-2.*ER*COSIKN
      BUG=(AA*R(M)+ER*COSIKN*GLCV)/ROOT(M)
      RTEMP=BUG/SQRT((AB+R(M)*(R(M)+BB))**3)
      ZTEMP=RTEMP
  651 RAT=RAT+GL(M,IWK)*EXK(K)*ZTEMP
      ZTEMP=VTEMP
   63 PTWK=PTWK+RAT*ZTEMP
      ZTFMP=CF*DELT/2.
      PTRL=PTRL*ZTEMP
      PTWK=PTWK*ZTEMP
      DO 46 M=1,MT
      GLCV=GLR(M)
      NVM=NVV(M)
      DO 46 I=1,NVM
      PHI=(I+NLE(M)-NL-2)*DELT
      AA=EX-GLCV*PHI
      AB=AA**2+ER**2
      DO 46 K=1,NBLADE
      ANGI=PHI+KD(K)-TETA
      SP=(0.-1.)*STEMP*(PHI+KD(K))
      BB=-2.*ER*COS(ANGL)
      AG=0.
      MD=M+1
```

```
      BUG=-1.
      DO 48  N=M,MD
      AH=2.0*(SQRT(RZSQ(N)+RZ(N)*BB+AB)+RZ(N)+
     1 .5*BB)
      AH=ABS(AH)
      AG=AG+BUG*ALOG(AH)
   48 BUG=-BUG
   46 PTSC=PTSC-AG*CEXP(SP)*SB(M,I)
      PTSC=PTSC*CF/2.
C
C  THIS SECTION OF THE MAIN PROGRAM FINDS THE FIELD POINT
C  PRESSURE AND DETERMINES ITS HARMONIC COMPONENTS
C
   96 PRS(ITETA)=20.2668*VS*((60.0/RPM)**2)/(DIAM**2)*
     1 (.5*DIAM*(PTBL+PTWK+PTSC)+1.6889*VFP*VS*(SOURCA+
     2 BOUNDA+BWAKEA+TRAILA+TWAKEA)+.65236*DIAM*RPM*ER*
     3 (SOURCT+BOUNDT+BWAKET+TRAILT+TWAKET))*CEXP(NHARM*
     4 ITETA*DTETA*(-.0*1.0))
      TM=.625*(ITETA-1)
      WRITE(6,91) TM,PRS(ITETA)
   91 FORMAT(/19X,F6.4,3X,F10.6,2X,F10.6)
      IF(ITETA.LT.8) GO TO 53
      DO 92 I=1,16
   92 NI(I)=(I-1)*NBLADE
      CALL HARM(PRS,NV,INV,SS,-1,IFERR)
      WRITE(6,93) (NI(I),PRS(I),I=1,8)
   93 FORMAT(1H1/24X,'2 - HARMONIC COMPONENTS'//
     1 17X,'HARM.NO.',13X,'KP'/
     2 31X,'REAL',8X,'IMAG'/
     3 (/2.X,I2,6X,F10.6,2X,F10.6))
      GO TO 41
   99 STOP
      END
```

```
BLOCK DATA
COMMON/Q3/NDK(199),IDK(66),Z(17),TK(17),XMP(10),NV(3)
DATA XMP/
A .05'526,..72273,1.04720,1.31812,1.57686,
B 1.82348,2.09439,2.41886,2.63623,3.14159/
DATA Z/
A ...0.0010,0.0025,0.005,0.01,0.02,0.03,0.04,
B .05,0.06,0.07,0.08,0.09,0.95,0.975,0.99,1.000/
DATA TK/
A .,0.189.,0.2932,0.4132,0.5814,0.8.,
B 0.9274,0.994.,0.9924,0.9306,0.8370,0.6220.
C .03754,0.2286,0.1496,0.998,0.0000/
DATA IDK/
A 2.,-1.10*5.10*10,10*20,15*60,.0/
DATA NDK/
A 6 1.4.,3.36*5.36*10,27*20/
DATA NV/
A 3.0.9/
END
```

```
      SUBROUTINE OUTPUT
C  PRINTS THE CHARACTERISTICS OF THE PROPELLER AND WAKE
C  AND THE LOADING COEFFICIENTS
C
      REAL KN
      COMPLEX A
      COMMON/QI/IDENT(18),XR(19),XSL(19),XST(19),XTZ(19),
     1 XTBETA(9),XVXN(9),XPHN(9),DIAM,DHUB,RPM,
     2 DELT,NBLADE,NHARM,MT/Q2/A(25,19),VX9(25),KN(25),
     3 VS,IGR,NMAX
      WRITE(6,1) IDENT,DIAM,DHUB,NBLADE,RPM,(XR(I),XSL(I),
     1 XST(I),XTZ(I),I=1,19)
    1 FORMAT(1H X,                  PRESSURE FIELD AROUND A MARINE',
     1  'PROPELLER                 '////
     2  26X,'PROPELLER CHARACTERISTICS'///
     3  19X,'TYPE',11X,18A4//
     4  19X,'DIAMETER',7X,F8.4,1X,'INCHES'//
     5  19X,'HUB DIAMETER',3X,F8.4,1X,'INCHES'//
     6  19X,'NO. OF BLADES',2X,I3//
     7  19X,'RPM',12X,F10.4///
     8  19X,'BLADE OUTLINE (UNITS-FRACTION OF RADIUS)'//
     9  21X,'RADII',3X,'LEAD.EDGE TRAIL.EDGE MAX.THICK.'/
     1 (/20X,F6.3,3X,F8.4,3X,F8.4,2X,F8.4))
      WRITE(6,15) MT,DELT
   15 FORMAT(////19X,'GRID SPACING'//
     1  19X,'NO. OF SPANWISE PANELS',6X,I3/
     2  19X,'ANGULAR CHORDWISE SPACING',3X,F10.7,2X,'RADIANS')
      WRITE(6,2) VS,NHARM,(XR(I),XVX0(I),XTBETA(I),XVXN(I),
     1 XPHN(I),I=1,9)
    2 FORMAT(1H1//27X,'INFLOW CHARACTERISTICS'///
     1  19X,'SYMBOLS AND UNITS'//
     2  19X,'VS',7X,'SHIP SPEED, KNOTS'/
     3  19X,'RADII',4X,'FRACTION OF RADIUS'/
     4  19X,'XVX0',5X,'ZEROTH HARMONIC OF INFLOW / VS'/
     5  19X,'TANBETA',2X,'TANGENT OF ADVANCE ANGLE'/
     6  19X,'NHARM',4X,'HARMONIC NUMBER'/
```

```
    7 19X,'XVXN',5X,'AMPLITUDE OF NHARM OF INFLOW / VS'/
    8 19X,'XPHN',5X,'PHASE OF NHARM OF INFLOW, RADIANS'//
    9 25X,'VS=',F8.4,3X,'NHARM=',I3//
    1 21X,'RADII',5X,'XVXL',4X,'TANBETA',5X,'XVXN',.
    2 5X,'XPHN'/
    3 (/7 X,F5.3,4(2X,F8.4)))
      IF(IGB.EQ.0.) GO TO 12
      WRITE(6,11)
   11 FORMAT(1H1//27X,'LOADING DISTRIBUTION'//
    1 20X,'(PRESSURE MODES)')
      GO TO 1
   12 WRITE(6,9)
    9 FORMAT(1H1//27X,'LOADING DISTRIBUTION'//
    1 28X,'(VORTICITY MODES)')
   13 WRITE(6,4) ((XR(J),I,A(J,I),I=1,NMAX),J=1,9)
    4 FORMAT(//21X,'RADII',4X,'MODE',13X,'COEF.'//
    1 41X,'REAL',8X,'IMAG.'//
    2 (2,X,F5.3,4X,I3,5X,F10.6,2X,F10.6))
      WRITE(6,13)
   13 FORMAT(1H1/23X,'*** PRESSURE FIELD RESULTS ***'///
    1 19X,'SYMBOLS AND UNITS'//
    2 19X,'EX',5X,'AXIAL COORDINATE OF FIELD POINT.'/
    3 26X,'FRACTION OF RADIUS'/
    4 19X,'EK',5X,'RADIAL COORDINATE OF FIELD POINT.'/
    5 26X,'FRACTION OF RADIUS'/
    6 19X,'TETA',3X,'ANGULAR COORDINATE OF FIELD POINT.'/
    7 26X,'RADIANS'/
    8 19X,'NT',5X,'NONDIMENSIONAL TIME, NT=TIME*RPM/60'/
    9 19Y,'KP',5X,'PRESSURE COEFF., P/(DENSITY*((RPM/
    1 26X,'60)*(DIAMETER**2)')
      RETURN
      END
```

```
      FUNCTION FILLIN(X,AB,OR,NO)

C  FINDS OR(X) BY PARABOLIC INTERPOLATION FROM TABLE OF
C  AB(N) AND OR(N) CONTAINING NO POINTS
C
      DIMENSION AB(2),OR(2)
      ANTRA(X1,X2,X3,X,Y1,Y2,Y3)=Y1*(X-X2)*(X-X3)/
     1 ((X1-X2)*(X1-X3))+Y2*(X-X1)*(X-X3)/((X2-X1)*
     2 (X2-X3))+Y3*(X-X1)*(X-X2)/((X3-X1)*(X3-X2))
      IF(X-AB(1))  1,3,2
    3 Y=OR(1)
      GO TO 99
    1 Y=ANTRA(AB(1),AB(2),AB(3),X,OR(1),OR(2),OR(3))
      GO TO 99
    2 IF(X-AB(2))1,6,5
    6 Y=OR(2)
      GO TO 99
    5 DO 7 I=3,NO
      M=I
      IF(X-AB(I))8,9,7
    9 Y=OR(I)
      GO TO 99
    7 CONTINUE
    8 Y=ANTRA(AB(M-2),AB(M-1),AB(M),X,OR(M-2),
     1 OR(M-1),OR(M))
   99 FILLIN=Y
      RETURN
      END
```

```
C     COMPLEX FUNCTION FITTIN(X,AB,OR,N,NO)
C
C SAME AS FILLIN BUT FOR TWO DIMENSIONAL, COMPLEX ARRAY
C
      COMPLEX ANTRA,OR(2,10),Y,Y1,Y2,Y3
      DIMENSION AB(2)
      ANTRA(X1,X2,X3,X,Y1,Y2,Y3)=Y1*(X-X2)*(X-X3)/
     1 ((X1-X2)*(X1-X3))+Y2*(X-X1)*(X-X3)/((X2-X1)*
     2 (X2-X3))+Y3*(X-X1)*(X-X2)/((X3-X1)*(X3-X2))
      IF(X-AB(1)) 1,3,2
    3 Y=OR(1,N)
      GO TO 99
    1 Y=ANTRA(AR(1),AB(2),AB(3),X,OR(1,N),OR(2,N),
     1 OR(3,N))
      GO TO 99
    2 IF(X-AR(2)) 1,6,5
    6 Y=OR(2,N)
      GO TO 99
    5 DO 7 I=3,NO
      M=I
      IF(X-AB(I)) 8,9,7
    9 Y=OR(I,N)
      GO TO 99
    7 CONTINUE
    8 Y=ANTRA(AB(M-2),AB(M-1),AB(M),X,OR(M-2,N),
     1 OR(M-1,N),OR(M,N))
   99 FITTIN=Y
      RETURN
      END
```

```
      COMPLEX FUNCTION BVORT(M,Y)
C
C  EVALUATES THE BOUND CIRCULATION IN THE PANEL M AT THE
C  ANGLE Y. HAS TWO OPTIONS: IF IGB=0 EVALUATES THE CIR-
C  CULATION DIRECTLY FROM THE INPUT DISTRIBUTION. IF IGB
C  > SOLVES A VOLTERRA EQUATION BASED ON THE INPUT PRE-
C  SSURE DISTRIBUTION.
C
      REAL KN
      COMPLEX A,RAT,CAT,MOUSE,SP,CEXP
      COMMON/Q2/A(25,10),VX5(25),KN(25),VS,IGB,NMAX
      BVORT=A(M,1)*(1.0+COS(Y))/SIN(Y)
      DO 14 N=2,NMAX
   14 BVORT=BVORT+A(M,N)*SIN((N-1)*Y)
      IF(IGB.GT.3) GO TO 13
      IF(KN(M).EQ.0.0) GO TO 16
      RAT=(3.0+1.0)*KN(M)
      RAT=-3.14159*RAT/(1.0+RAT)*(A(M,1)+0.5*A(M,2))
      BVORT=BVORT+0.5*RAT*(1.0-COS(Y))
      GO TO 16
   13 IF(KN(M)) 16,16,11
   1. BVORT=BVORT/(VX2(M)*VS*1.6889)
      GO TO 16
   11 BUG=1.0
      SP=(0.0,1.0)*KN(M)
      RAT=SP
      CAT=SP
      K=1
      N=3
   36 N=N+1
      BUG=-BUG
      CAT=CAT*SP
      K=K*N
      MOUSE=BUG*CAT*(COS(Y)**N)/K
      RAT=RAT+MOUSE
      IF(CABS(MOUSE/RAT).LT.0.001) GO TO 37
```

```
      IF(N.GT.14) GO TO 37
      GO TO 36
   37 MOUSE=A(M.1)*(Y-SIN(Y))+A(M,2)*(Y/2.0-0.25*
     1 SIN(2*Y))
      IF(NMAX.LT.3) GO TO 40
      DO 39 N=3,NMAX
   39 MOUSE=MOUSE+0.5*A(M.N)*(SIN((N-2)*Y)/(N-2)-
     1 SIN(N*Y)/N)
   4. BVORT=(BVORT-RAT*CEXP(-SP)*MOUSE)/(VX0(M)*VS#1.6889)
   16 RETURN
      END
```

```
      COMPLEX FUNCTION FWA(X)
C  SETS THE INTEGRAND FOR THE STREAMWISE INTEGRATION OF THE
C  AXIAL VELOCITY DUE TO THE TRAILING VORTICES WHEN NHARM>0
C
      COMPLEX CEXP
      COMMON/Q4/KK,DK,XU,EP,EX,TETA,ALFA,GLCV,AR
      ANGL=Y+ALFA+KK*YU
      COSIKN=COS(ANGL+DK-TETA)
      BB=-2.*ER*COSIKN
      AA=FX-GLCV*ANGL
      AR=AA**2+ER**2
      BUG=SQRT((AR+BB*AR+AR**2)**3)
      FWA=AR*(AR-ER*COSIKN)/BUG*CEXP((0.,-1.)*3.14159/XU*
     1 (X+ALFA))
      RETURN
      END
```

```
      COMPLEX FUNCTION FWT(X)
C  SETS THE INTEGRAND FOR THE STREAMWISE INTEGRATION OF THE
C  TANGENTIAL VELOCITY DUE TO THE TRAILING VORTICES WHEN NHARM>0
C
      COMPLEX CEXP
      COMMON/Q4/KK,DK,XU,ER,EX,TETA,ALFA,GLCV,AR
      ANGL=X+ALFA+KK*XU
      COSIKN=COS(ANGL+DK-TETA)
      SINIKN=SIN(ANGL+DK-TETA)
      BB=-2.*ER*COSIKN
      AA=EX-GLCV*ANGL
      AB=AA**2+ER**2
      BUG=SQRT((AB+BB*AR+AR**2)**3)
      FWT=(-AR*(GLCV*COSIKN-AA*SINIKN)+ER*GLCV)/BUG*
     1 CEXP((0.,-1.)*3.14159/XU*(X+ALFA))
      RETURN
      END
```

```
      SUBROUTINE QG5(XL,XU,FCT,Y)
C FIVE POINT GAUSSIAN QUADRATURE
C
      COMPLEX FCT,Y
      A=.5*(XU+XL)
      B=XU-XL
      C=.4530899*B
      Y=.1184634*(FCT(A+C)+FCT(A-C))
      C=.2692347*B
      Y=Y+.2303143*(FCT(A+C)+FCT(A-C))
      Y=B*(Y+.2844444*FCT(A))
      RETURN
      END
```